

Pattern Formation Problem for Synchronous Mobile Robots in the Three Dimensional Euclidean Space

Yukiko Yamauchi ^{*}, Taichi Uehara, and Masafumi Yamashita

Kyushu University, Japan.

Abstract. Self-organization of a swarm of mobile computing entities in the three-dimensional Euclidean space (3D-space) such as drones and satellites attracts much attention as such systems are required to accomplish more complicated tasks. We consider a swarm of autonomous mobile robots each of which is an anonymous point in 3D-space and synchronously executes a common distributed algorithm. We investigate the *pattern formation problem* that requires the robots to form a given target pattern from an initial configuration and characterize the problem by showing a necessary and sufficient condition for the robots to form a given target pattern.

The pattern formation problem in the two dimensional Euclidean space (2D-space) has been investigated by Suzuki and Yamashita (SICOMP 1999, TCS 2010), and Fujinaga et al. (SICOMP 2015). The symmetricity $\rho(P)$ of a configuration (i.e., the positions of robots) P is the order of the cyclic group that acts on P with the exception that when a robot is on the center of the smallest enclosing circle of P , $\rho(P) = 1$. It has been shown that fully-synchronous (FSYNC) robots can form a target pattern F from an initial configuration P if and only if $\rho(P)$ divides $\rho(F)$.

We extend the notion of symmetricity to 3D-space by using the *rotation groups* each of which is defined by a set of rotation axes and their arrangement. We define the symmetricity $\varrho(P)$ of configuration P in 3D-space as the set of rotation groups that acts on P and whose rotation axes do not contain any robot. We show the following necessary and sufficient condition for the pattern formation problem which is a natural extension of the existing results of the pattern formation problem in 2D-space: FSYNC robots in 3D-space can form a target pattern F from an initial configuration P if and only if $\varrho(P) \subseteq \varrho(F)$. This result guarantees that, for example, from an initial configuration where the robots form a cube (i.e., the robots occupy the vertices of a cube), they can form a regular octagon that consists of points on a plane or a square anti-prism that has a vertical axis. In other words, these target patterns have lower symmetry than the initial configuration. For solvable instances, we present a pattern formation algorithm for oblivious FSYNC robots. The insight of this paper is that symmetry of mobile robots in 3D-space is sometimes lower than the symmetry of their positions and the robots can show their symmetry by their movement.

Keywords. Mobile robots in the three dimensional Euclidean space, pattern formation, rotation group, symmetry breaking.

^{*} Corresponding author. Address: 744 Motooka, Nishi-ku, Fukuoka 819-0395, Japan. Fax: +81-92-802-3637. Email: yamauchi@inf.kyushu-u.ac.jp

1 Introduction

Distributed control of a system consisting of autonomous mobile computing entities in the three dimensional Euclidean space (3D-space) is one of the most challenging problems in distributed computing theory and robotics. One of the most important properties that is expected to such systems is *self-organization ability* that enables the system to obtain the coordination by itself. For example, drones are becoming widely available and their applications in sensing, monitoring, and rescuing in harsh environment such as disaster area and active volcanoes, where they are required to coordinate themselves without human intervention, are attracting much attention.

As one of the most fundamental tasks in 3D-space, this paper considers the *pattern formation problem* that requires a swarm of robots to form a given 3D target pattern. A robot is a point in 3D-space that autonomously moves according to a given rule. We adopt the conventional computation model [14, 17, 18], i.e., each robot repeats a Look-Compute-Move cycle, where it observes the positions of other robots (Look phase), computes its next position with a given algorithm (Compute phase), and moves to the next position (Move phase). Each robot is *anonymous* in the sense that they have no identifiers and the robots are *uniform* in the sense that all robots execute a common algorithm. Each robot has no access to the global x - y - z coordinate system (like GPS) and its observation and movement are done in terms of its *local x - y - z coordinate system*. The origin of the local coordinate system of a robot is its current position and the local coordinate system has arbitrary directions and unit distance. However we assume that all local coordinate systems are right-handed. Thus each local coordinate system is either a uniform scaling, transformation, rotation, or their combination of the global coordinate system. A robots is *oblivious* if its local memory is refreshed at the end of each cycle, otherwise *non-oblivious*. Hence the input to the algorithm at an oblivious robot is the observation obtained in the current cycle. Suzuki and Yamashita pointed out that oblivious mobile robot system is self-stabilizing [8], that guarantees self-organization and fault tolerance against finite number of transient faults [17]. In a Move phase, each robot reaches the next position and in this paper we do not care for the track of movement.¹ We consider the *fully-synchronous (FSYNC)* model where the robots execute the t -th Look-Compute-Move cycle at the same time with each of the Look, Compute, and Move phases completely synchronized. Here a *configuration* of the robots is the positions of the robots observed in the global coordinate system. These assumptions mean that the robots do not have explicit communication medium and they have to tolerate inconsistency among local coordinate systems so that they coordinate themselves by building some agreement by using inconsistent observations.

The pattern formation problem was first introduced by Suzuki and Yamashita for the robots moving in the two-dimensional Euclidean space (2D-space) [17]. They characterized the class of formable patterns by using the notion of *symmetricity* of an initial configuration. The symmetricity of a configuration is essentially the order of the cyclic group that acts on it. Let P be an initial configuration of robots without any multiplicity.² We consider the decomposition of P into regular m -gons centered at the center of the smallest enclosing circle of P . The symmetricity $\rho(P)$ of P is the maximum value of such m with an exception that when a single point of P is at the center of the smallest enclosing circle of P , $\rho(P) = 1$. We consider a point as a regular 1-gon with an

¹ This type of movement is called rigid movement. On the other hand, non-rigid movement allows a robot to stop en route after moving unknown minimum moving distance δ in a Move phase. If the track to the next position is shorter than δ , non-rigid movement makes a robot stop at the next position.

² Throughout this paper, we assume that any initial configuration contains no multiplicity. It is impossible to break up multiple robots on a single position as we assume all robots execute the same algorithm.

arbitrary center and a set of two points as a regular 2-gon with the center at the midpoint of the two points. This exception is derived from an easy symmetry breaking algorithm, i.e., the robot on the center leaves its current position. Then they showed that FSYNC robots can form a target pattern F from a given initial configuration P if and only if $\rho(P)$ divides $\rho(F)$ regardless of obliviousness. This impossibility is by the fact that since $\rho(P)$ divides the robots into regular $\rho(P)$ -gons, these symmetric $\rho(P)$ robots cannot break their symmetry. Thus robots in 2D-space cannot break rotational symmetry of an initial configuration.

Yamauchi et al. first showed that rotational symmetry of robots in 3D-space causes the same impossibility [21]. They considered the *plane formation problem* that requires the robots to land on a common plane without making any multiplicity. In 3D-space, there are five-kinds of rotation groups with finite order, i.e., *the cyclic groups, the dihedral groups, the tetrahedral group, the octahedral group, and the icosahedral group* [2, 4, 5]. Given a configuration P in 3D-space, its *rotation group* $\gamma(P)$ is the rotation group that acts on P and none of its supergroup in these five kinds of rotation groups acts on P . They called the cyclic groups and the dihedral groups *two-dimensional (2D)*, while the remaining three rotation groups *three-dimensional (3D)*, because 3D rotation groups do not act on points on a plane. Then they showed that the robots cannot form a plane from an initial configuration P if and only if $\gamma(P)$ is a 3D rotation group and all robots are not on the rotation axes of $\gamma(P)$. The results showed that even when the robots form a regular polyhedron (except an regular icosahedron) in an initial configuration, they can break their 3D rotation group and form a plane.

In this paper, we define the *symmetricity* $\varrho(P)$ of a configuration P in 3D-space as a set of rotation groups that acts on the positions of robots and that consists of rotation axes containing no robot. We will give the following necessary and sufficient condition for the pattern formation problem in 3D-space.

Theorem 1. *Regardless of obliviousness, FSYNC robots can form a target pattern F from an initial configuration P if and only if $\varrho(P) \subseteq \varrho(F)$.*

The impossibility is derived from symmetry among robots in the same way as 2D-space. For the solvable instances, we present a pattern formation algorithm for oblivious FSYNC robots that non-oblivious robots can execute correctly by just ignoring its memory contents. Theorem 1 guarantees, for example, that the robots can form a square anti-prism or a regular octagon from an initial configuration where they form a cube, because their symmetricity is identical while the rotation groups of the target patterns are dihedral and that of the initial configuration is the octahedral group. Thus the rotation group of the robots decreases during the formation. (See Figure 1.) We will show that the robots can translate a given initial configuration P into another configuration P' with $\gamma(P') \in \varrho(P)$. From the definition, $\gamma(P') \preceq \gamma(P)$. The symmetry breaking algorithm is based on the “go-to-center” algorithm proposed in [21]. Theorem 1 guarantees that such $\gamma(P')$ is an element of $\varrho(F)$ which means that $\gamma(P')$ is a subgroup of $\gamma(F)$. We will show that the robots can easily form F from such P' by embedding an image of F into P' and building an agreement on a perfect matching between F and P' .

The main contribution of this paper is the fact that the symmetry of moving points is different from symmetry of their positions and robots can show their symmetry by their movement. We finally note that our result is a generalization of existing results for FSYNC robots in 2D-space [17].

Related work. The only existing paper on autonomous mobile robot systems in 3D-space [21] considers the plane formation problem motivated by the fact that autonomous mobile robot systems in 2D-space has been extensively investigated. We mainly survey the results on formation problems

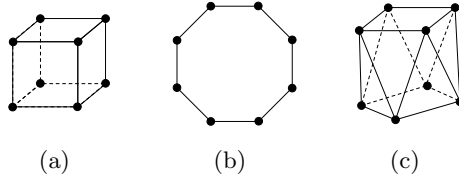


Fig. 1. Example of an initial configuration and target patterns with the same symmetricity. (a) Initial configuration P where robots form a cube and $\gamma(P)$ is the octahedral group. (b)(c) Target patterns F and F' where robots form a regular octagon and a regular square anti-prism. Thus $\gamma(F)$ and $\gamma(F')$ are dihedral groups.

in 2D-space. The main research interest has been the computational power of robot systems and minimum requirements for the robots to accomplish a given task. Many fundamental distributed tasks have been introduced, for example, *gathering* [17], *pattern formation* [17], *partitioning* [9], *covering* [15], and so on. The book by Flocchini et al. [10] contains almost all results on autonomous mobile robot systems up to year 2012.

Asynchrony among robots is classified into three models; the fully synchronous (FSYNC) model, the *semi-synchronous* (SSYNC) model, and the *asynchronous* (ASYNC) model. The robots are SSYNC if some robots do not start the i -th Look-Compute-Move cycle for some i , but all robots that have started the cycle synchronously execute their Look, Compute, and Move phases [17]. The robots are ASYNC if no assumptions are made on the execution of Look-Compute-Move cycles [13].

Yamashita et al. characterized the pattern formation problem for each of the FSYNC, SSYNC, and ASYNC models [14, 17, 18], that are summarized as follows: (1) For non-oblivious FSYNC robots, pattern F is formable from an initial configuration P if and only if $\rho(P)$ divides $\rho(F)$. (2) Pattern F is formable from P by oblivious ASYNC (thus SSYNC) robots if F is formable from P by non-oblivious FSYNC robots, except for F being a point of multiplicity 2.

This exceptional case is called the rendezvous problem. Indeed, it is trivial for two FSYNC robots, but it is unsolvable for two oblivious SSYNC (and hence ASYNC) robots while oblivious SSYNC (and ASYNC) robots can converge to a point [17]. However, more than two robots can form a point in the SSYNC model [17] and in the ASYNC model [3]. In terms of symmetricity, the point formation problem is one of the easiest problems (except the rendezvous problem), since $\rho(F) = n$ when F is a point of multiplicity n and $\rho(P)$ is always a divisor of n by the definition of the symmetricity, where n is the number of robots.

The other easiest case is a regular n -gon, which is also called the circle formation problem, since $\rho(F) = n$. Recently the circle formation problem for n oblivious ASYNC robots ($n \neq 4$) is solved without agreement of clockwise direction, i.e., chirality [11].

Yamauchi et al. showed a randomized pattern formation algorithm for oblivious ASYNC robots that breaks the symmetricity of the initial configuration and forms any target pattern with probability 1 [20].

The notion of *compass* was first introduced in [12] that assumes agreement of the direction and/or the orientation (i.e., the positive direction) of x - y local coordinate systems. Flocchini et al. showed that if oblivious ASYNC robots agree on the directions and orientations of x - y axes, they can form any arbitrary target pattern [13].

Das et al. characterized the formation of a sequence of patterns by oblivious SSYNC robots in terms of symmetricity [7]. They showed that symmetricity of each pattern of a formable sequence

should be identical and a multiple of the symmetricity of an initial configuration. Such sequence of patterns is a geometric global memory formed by oblivious robots.

All above results are based on unlimited visibility of robots. A robot has *limited visibility* if it can observe other robots within the unknown fixed visibility range [12]. Yamauchi et al. showed that oblivious FSYNC (thus SSYNC and ASYNC) robots with limited visibility have substantially weaker formation power than FSYNC robots with unlimited visibility [19]. Ando et al. proposed a convergence algorithm for oblivious SSYNC robots with limited visibility [1] while Flocchini et al. assumed consistent compass for convergence of oblivious ASYNC robots with limited visibility [12].

Peleg et al. first introduced the *luminous robot model* where each robot is equipped with externally and/or internally visible lights [16]. Das et al. provided an algorithms for oblivious luminous robots to simulate robots without lights in stronger synchronization model and showed that two ASYNC (thus SSYNC) luminous robots can form a point [6].

Organization. We define the mobile robot model in Section 2 and we introduce the rotation groups and symmetricity of a configuration in Section 3. Then we show that the robots can reduce their rotation group to some element of the symmetricity of an initial configuration by the “go-to-center” algorithm in Section 4. We prove the necessity of Theorem 1 in Section 5 and sufficiency of Theorem 1 in Section 6 by showing a pattern formation algorithm for oblivious FSYNC robots. Finally Section 7 concludes this paper.

2 Preliminary

Let $R = \{r_1, r_2, \dots, r_n\}$ be a set of $n \geq 3$ robots each of which is represented by a point in 3D-space. Each robot is anonymous and there is no way to distinguish them. We use the indexes just for description.

By Z_0 we denote the global x - y - z coordinate system. Let $p_i(t) \in \mathbb{R}^3$ be the position of r_i at time t in Z_0 , where \mathbb{R} is the set of real numbers. A *configuration* of R at time t is denoted by a multiset $P(t) = \{p_1(t), p_2(t), \dots, p_n(t)\}$. Let $\mathcal{P}_n^3 = (\mathbb{R}^3)^n$ be the set of all configurations. We assume that the robots initially occupy distinct positions, i.e., $p_i(0) \neq p_j(0)$ for all $1 \leq i < j \leq n$.³ The robots have no access to Z_0 . Instead, each robot r_i observes the positions of other robots in its local x - y - z coordinate system Z_i , where the origin is always its current position, while the direction of each positive axis and the magnitude of the unit distance are arbitrary but never change.⁴ We assume that Z_0 and all Z_i are right-handed. Thus Z_i is either a uniform scaling, transformation, rotation, or their combinations of Z_0 . By $Z_i(p)$ we denote the coordinates of a point p in Z_i .

We consider discrete time $0, 1, 2, \dots$ and at each time step the robots execute a Look-Compute-Move cycle with each of Look, Compute, and Move phases completely synchronized, i.e., we consider the *fully-synchronous (FSYNC)* robots in this paper. We specifically assume without loss of generality that the $(t+1)$ -th Look-Compute-Move cycle starts at time t and finishes before time $t+1$. At time t , each $r_i \in R$ obtains a multiset $Z_i(P(t)) = \{Z_i(p_1(t)), Z_i(p_2(t)), \dots, Z_i(p_n(t))\}$ in the Look phase. We call $Z_i(P(t))$ the *local observation* of r_i at t . Then r_i computes its next position using an algorithm ψ , which is common to all robots. If ψ uses only $Z_i(P(t))$, we say that r_i is *oblivious*. Otherwise, we say r_i is *non-oblivious*, i.e., r_i can use past local observations and past outputs of ψ .

³ This assumption is necessary because it is impossible to break up multiple oblivious FSYNC robots (with the same local coordinate system) on a single position as long as they execute the same algorithm. The proposed pattern formation algorithm does not make any multiplicity during the formation. However, we have to consider configurations with multiplicity when we prove impossibility by checking executions of any arbitrary algorithm.

⁴ Since Z_i changes whenever r_i moves, notation $Z_i(t)$ is more rigid, but we omit parameter t to simplify its notation.

Finally, r_i moves to $\psi(Z_i(P(t)))$ in Z_i before time $t + 1$. Thus the movement of robots is *rigid*. In this paper, we do not care for the track of the movement of robots, rather each robot jumps to its next position. An infinite sequence of configurations $\mathcal{E} : P(0), P(1), \dots$ is called an *execution* from an *initial configuration* $P(0)$. Observe that the execution \mathcal{E} is uniquely determined, once initial configuration $P(0)$, local coordinate systems of robots at time 0, initial local memory contents (if any), and algorithm ψ are fixed.

Pattern formation problem. The *pattern formation problem* is to make the robots form a given target pattern F from an initial configuration P . The target pattern F is given to each robot as a set of coordinates of n points in Z_0 . We assume that F does not contain any multiplicity, but as we will discuss in Section 7, we can easily extend the results to target patterns with multiplicities. Because robots do not have access to the global coordinate system, it is impossible to form F itself. Let \mathcal{T} be the set of all rotations, translations, uniform scalings, and their combinations. We say F' is *similar* to F if there exists $Z \in \mathcal{T}$ such that $F' = Z(F)$, which we denote by $F' \simeq F$. We say that the robots form a target pattern F from an initial configuration P , if, regardless of the choice of local coordinate systems and memory contents (if any) of robots in the initial configuration, any execution $P(0)(= P), P(1), \dots$ reaches a configuration $P(t)$ that is similar to F in finite time.

For any (multi-)set of points P , by $B(P)$ and $b(P)$, we denote the *smallest enclosing ball* of P and its center, respectively. A point on the sphere of a ball is said to be *on* the ball and we assume that the *interior* or the *exterior* of a ball does not include its sphere. The *innermost empty ball* $I(P)$ of P is the ball centered at $b(P)$ and contains no point of P in its interior, but contains at least one point of P on it. When all points are on $B(P)$, we say that P is *spherical*. Given a ball B , $rad(B)$ denotes the radius of B . We denote a ball centered at an arbitrary point b and with radius r by $Ball(b, r)$.

3 Symmetricity in 3D-Space

In this section, we define the *rotation group* and the *symmetricity* of a set of points and investigate the relation between the two notions. We start with an arbitrary set of points because any initial configuration and any target pattern contain no multiplicity, and then extend these notions to multiset of points since we should consider an arbitrary algorithm that may produce multiplicity when we discuss impossibility.

In 2D-space, the symmetricity $\rho(P)$ of a configuration P considers the worst-case arrangement of local coordinate system of P , that is caused by the rotations around the center of the smallest enclosing circle of P , denoted by $c(P)$, i.e., the *cyclic group* of order $\rho(P)$. Hence $\rho(P)$ is redefined as follows: For an initial configuration P identified as a set of points, $\rho(P)$ is the maximum order of the cyclic group that acts on P with the exception such that when $c(P) \in P$, $\rho(P) = 1$. This exceptional case means that whenever $c(P) \in P$, the robot on $c(P)$ can translate P into another asymmetric configuration P' with $\rho(P') = 1$ by leaving $c(P)$ which is on the rotation axes of the cyclic group.

In 3D-space, we consider rotation groups so that we check all possible symmetric arrangement of local coordinate systems. There are only five kinds of finite-order rotation groups in 3D-space; the cyclic groups, the dihedral groups, the tetrahedral group, the octahedral group, and the icosahedral group.⁵ Symmetry operations in 3D-space consist of rotation around an axis, reflection for a mirror plane (bilateral symmetry), reflections for a point (central inversion), and rotation-reflections .

⁵ These five kinds of groups are proper subgroup of $SO(3)$, which is defined by rotations of a unit ball and its order is infinite

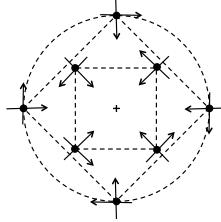


Fig. 2. A symmetric initial configuration in 2D-space, whose symmetricity is 4. Eight robots and their local coordinate systems are symmetric with respect to the center of their smallest enclosing circle. There are two groups consisting of 4 symmetric robots and the robots in each group cannot break their symmetry.

However, we consider symmetry among robots, specifically, whether the robots have identical local observation or not. Because all local coordinate systems are right-handed, it is sufficient to consider transformations that preserve the center of the smallest enclosing ball of robots and keep Euclidean distance and handedness, in other words, direct congruent transformations. Such symmetry operations consist of rotations around some axes and we consider above five kinds of rotation groups. (See, for example, [4, 5] for more detail.)

In the following, we first define the rotation group $\gamma(P)$ of a set of points P , which is the symmetry that the robots can agree by just observing P in their local coordinate systems. Then we define the rotation group $\sigma(P)$ of the arrangement of local coordinate systems of P , which is the symmetry that the robots can never break. However, the robots do not agree on $\sigma(P)$ by just observing the set of points P in their local coordinate systems. We define the symmetricity $\varrho(P)$ of P that consists of all possible rotation groups of the arrangement of local coordinate systems of P . Intuitively the maximal elements in $\varrho(P)$ are the worst-case symmetry of the robots. The maximality of $G \in \varrho(P)$ means that there is no proper supergroup of G in $\varrho(P)$ and $\varrho(P)$ actually has multiple such maximal elements. Based on these notions, we present the first impossibility result that shows that FSYNC robots can never reduce $\sigma(P)$ of an initial configuration P by any arbitrary algorithm.

3.1 Rotation group of a set of points

We formally define the five kinds of rotation groups. The rotation group $SO(3)$ has five kinds of subgroups of finite order [4, 5]; the cyclic groups C_k ($k = 1, 2, \dots$), the dihedral groups D_ℓ ($\ell = 2, 3, \dots$), the tetrahedral group T , the octahedral group O , and the icosahedral group I . Each of these groups is identified by the rotations of a regular pyramid with a regular k -gon base, a regular prism with regular ℓ -gon bases, a regular tetrahedron, a regular octahedron, and a regular icosahedron, respectively. (See Figure 3.) For example, consider a regular pyramid that has a regular k -gon as its base. The rotation operations for this regular pyramid are rotations by $2\pi i/k$ for $i = 1, 2, \dots, k$ around an axis containing the apex and the center of the base. We call such an axis k -fold axis. Let a^i be the rotation by $2\pi i/k$ around this k -fold axis with $a^k = e$ where e is the identity element. Then, a^1, a^2, \dots, a^k form the cyclic group C_k .

A regular prism (except a cube) has two parallel regular ℓ -gons as its top and bottom bases and has two types of rotation axes, one is the ℓ -fold axis containing the centers of its top and bottom bases, and the others are ℓ 2-fold axes that exchange the top and the bottom. We call this ℓ -fold axis *principal axis* and the remaining ℓ 2-fold axes *secondary axes*. These rotation operations on a

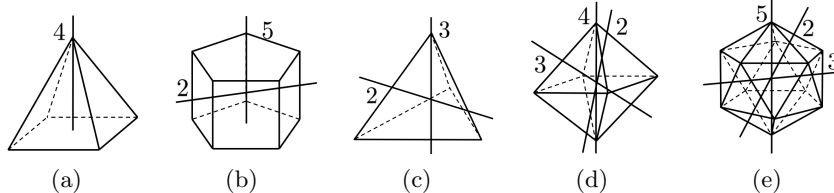


Fig. 3. Rotation groups. (a) the cyclic group C_4 , (b) the dihedral group D_5 , (c) the tetrahedral group T , (d) the octahedral group O , and (e) the icosahedral group I . Figures show only one axis for each fold of axes.

Table 1. Three polyhedral groups. The number of elements around k -fold axes excluding the identity element is shown. The number in the brackets is the number of rotation axes.

Polyhedral group	2-fold axes	3-fold axes	4-fold axes	5-fold axes	Order
T	3(3)	8(4)	-	-	12
O	6(6)	8(4)	9(3)	-	24
I	15(15)	20(10)	-	24(6)	60

regular prism form the *dihedral group* D_ℓ . When $\ell = 2$, we can define D_2 in the same way but in the group theory we do not distinguish the principal axis.

The remaining three rotation groups T , O , and I are called the polyhedral groups. Table 1 shows the number of rotation axes and the number of elements around each type of rotation axes for each of the polyhedral groups.

Let $\mathbb{S} = \{C_k, D_\ell, T, O, I \mid k = 1, 2, \dots, \text{and } \ell = 2, 3, \dots\}$ be the set of rotation groups, where C_1 is the rotation group with order 1; its unique element is the identity element (i.e., 1-fold rotation).

When G' is a subgroup of G ($G, G' \in \mathbb{S}$), we denote it by $G' \preceq G$. If G' is a proper subgroup of G (i.e., $G' \neq G$), we denote it by $G' \prec G$. For example, we have $T \prec O$, $T \prec I$, but $O \not\prec I$. If $G \in \mathbb{S}$ has a k -fold axis, then $C_k \preceq G$. Clearly, $C_{k'} \preceq C_k$ if $k' \mid k$, i.e., k' divides k , which also holds for dihedral groups. The relation \prec is asymmetric and transitive. Figure 4 shows the structure of subgroups of polyhedral groups.

For a set of points P , we consider rotations on P that produces P itself.

Definition 1. Let $P \in \mathcal{P}_n^3$ be a set of points. The rotation group $\gamma(P)$ of P is the rotation group in \mathbb{S} that acts on P and none of its proper supergroup in \mathbb{S} acts on P .

Clearly, if $\gamma(P) \succ C_1$, all rotation axes of $\gamma(P)$ contain $b(P)$, which is the single intersection of them. From the definition, we can uniquely determine $\gamma(P)$ irrespective of (local) coordinate system to observe P . For example, when P forms a regular pyramid with a regular square base, $\gamma(P) = C_4$, when P forms a square, $\gamma(P) = D_4$, and when P forms a cube, $\gamma(P) = O$. When the robots are on a line and symmetric against $b(P)$, $\gamma(P) = D_\infty$, and $\gamma(P) = C_\infty$ if they are asymmetric against $b(P)$.

We say a rotation axis of $\gamma(P)$ is *occupied* when it contains some points of P and *unoccupied* otherwise. For example, when P forms a cube, all 3-fold axes of $\gamma(P) = O$ are occupied while all 2-fold axes and all 4-fold axes are unoccupied.

In the group theory, we do not distinguish the principal axis of D_2 from the other two 2-fold axes. Actually, since we consider the rotations on a set of points in 3D-space, we can recognize a principal axis of D_2 . Consider a sphenoid consisting of 4 congruent triangles (Figure 5). A rotation axis of such a sphenoid contains the midpoints of opposite edges and there are three 2-fold axis

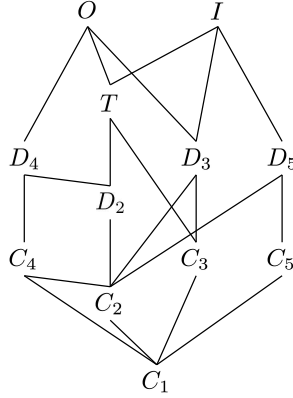


Fig. 4. The subgroups of polyhedral groups. Two groups G and G' are linked by a line if there is no proper subgroup G'' of G that satisfies $G' \prec G''$, and G is put above G' .

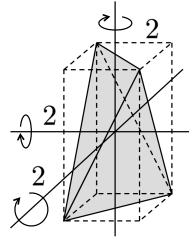


Fig. 5. A sphenoid consisting of 4 congruent triangles. Its rotation group is D_2 . Since the vertices are not placed equidistant positions from the three axes, we can distinguish an axis as the principal axis from the others.

perpendicular to each other. Hence the rotation group of such a sphenoid is D_2 . However we can recognize, for example, the vertical 2-fold axis from the others by their lengths (between the midpoints connecting). The polyhedra on which only D_2 can act are rectangles and the family of such sphenoids, and we can always recognize the principal axis. Other related polyhedra are squares and regular tetrahedra, but D_4 also acts on a square and T acts on a regular tetrahedron. Hence their rotation groups are proper supergroup of D_2 . We can show the following property regarding the principal axis of D_2 . See Appendix A for the proof.

Property 1. Let $P \in \mathcal{P}_n^3$ be a set of points. If D_2 acts on P and we cannot distinguish the principal axis of (an arbitrary embedding of) D_2 , then $\gamma(P) \succ D_2$.

Given a set of points P , $\gamma(P)$ determines the arrangement of its rotation axes in P . We thus use $\gamma(P)$ and its arrangement in P interchangeably. If $\gamma(P) = C_k$ ($k > 1$), the single rotation axis of C_k has a “direction” in the sense that P is asymmetric against $b(P)$. (Otherwise, $\gamma(P)$ is D_k .) An example is when P forms a pyramidal frustum with regular k -gon bases which we cannot rotate to exchange the top and bottom bases. We say the single rotation axis of C_k is *oriented*. The secondary axes of D_ℓ ($\ell > 2$) are oriented if ℓ is odd, otherwise not oriented. This is because the only rotation axis perpendicular to each secondary axis is the principal axis that has a π rotation if ℓ is even, and there is no such rotation axis, if ℓ is odd. Additionally, the 3-fold axes of T are oriented. Remember that D_3 is not a subgroup of T . On the other hand, 2-fold axis of T are not

oriented because D_2 is a subgroup of T . The rotation axes of O and I are not oriented because each rotation axes has at least one 2-fold axes that is perpendicular to it.

Embedding of a rotation group. We define an embedding of a rotation group to an arrangement of its supergroup. For two groups $G, H \in \mathbb{S}$, an *embedding* of G to H is an embedding of each rotation axis of G to one of the rotation axes of H so that any k -fold axis of G overlaps a k' -fold axis of H satisfying $k|k'$ with keeping the arrangement. If rotation axes of H are oriented, the corresponding rotation axes of G should keep the orientation. If the rotation axes of H are not oriented, we do not care for the orientation of G . For example, we can embed T to O so that each 3-fold axis of T overlaps a 3-fold axis of O and each 2-fold axis of T overlaps a 4-fold axis of O . Note that there may be many embeddings of G to H . There are six embeddings of C_4 to O depending on the choice of the 4-fold axis and its orientation. Observe that we can embed G to H if and only if $G \preceq H$.

Transitivity. We say that a set of points P is *transitive* regarding a rotation group G if it is an orbit of G through some seed point s , i.e., $P = Orb(s) = \{g * s \in P : g \in G\}$ for some $s \in P$.⁶ For a transitive set of points P and any $p \in P$, we call $\mu(p) = |\{g \in G : g * s = p\}|$ the *folding* of p .⁷ We of course count the identity element of G for $\mu(p)$ and $\mu(p) \geq 1$ holds for all $p \in P$. If $p \in P$ is at $b(P)$, its folding is $|\gamma(P)|$ and if p is on a k -fold axis of $\gamma(P)$, its folding is k . We have the following lemma.

Lemma 1. [21] *Let P be the transitive set of points generated by a rotation group $G \in \mathbb{S}$ and a seed point $s \in \mathbb{R}^3$. If $p \in P$ is on a k -fold axis of G for some k , so are the other points $q \in P$ and $\mu(p) = \mu(q) = k$ holds. Otherwise, if $p \in P$ is not on any axis of G , so are the other points $q \in P$, and $\mu(p) = \mu(q) = 1$ holds.*

Hence $\mu(p)$ for $p \in P$ is identical for a transitive set of points P generated by a rotation group G and a seed point s . We abuse μ to a transitive set of points P and $\mu(P)$ represents $\mu(p)$ for $p \in P$. When $\mu(P) > 1$, the positions of points of P is uniquely determined in the arrangement of G if we ignore uniform scalings that keep the center of G . Additionally, we have $|P| = |G|/\mu$. Table 2 shows the set of points generated by the five kinds of rotation groups.

$\gamma(P)$ -decomposition of P . Yamauchi et al. showed that a set of points P can be decomposed into transitive subsets [21]: For a point $p \in P$, let $Orb(p) = \{g * p \in P : g \in \gamma(P)\}$ be the orbit of the group action of $\gamma(P)$ through p . Then we let $\{P_1, P_2, \dots, P_m\} = \{Orb(p) : p \in P\}$ be its orbit space. From the definition, each P_i is transitive regarding $\gamma(P)$ and $\{P_1, P_2, \dots, P_m\}$ is a partition of P . Such partition is unique and we call it the *$\gamma(P)$ -decomposition* of P . Clearly, each element of the $\gamma(P)$ -decomposition is one of the polyhedron for $\gamma(P)$ shown in Table 2. Note that the sizes of the elements of the $\gamma(P)$ -decomposition of P may be different. The $\gamma(P)$ -decomposition of P does not depend on the local coordinate systems and each robot can recognize it.

For the $\gamma(P)$ -decomposition $\{P_1, P_2, \dots, P_m\}$ of P , we denoted the ball centered at $b(P)$ and contains P_i on it by $Ball(P_i)$ for each $1 \leq i \leq m$.

In [21], the authors showed the following theorem.

Theorem 2. [21] *Let $P \in \mathcal{P}_n^3$ be a configuration of robots recognized as a set of points. Then P can be decomposed into subsets $\{P_1, P_2, \dots, P_m\}$ in such a way that each P_i is a transitive set of points regarding $\gamma(P)$. Furthermore, the oblivious FSYNC robots can agree on a total ordering among the elements of the $\gamma(P)$ -decomposition of P .*

⁶ For a transitive set of points P , arbitrary point $s \in P$ can be a seed point.

⁷ In group theory, the folding of a point P is the size of the stabilizer of p defined by $G(p) = \{g \in G : g * p = p\}$ [2].

Table 2. The folding of seed points and transitive sets of points

Rotation Group	Order	Folding	Cardinality	Polyhedron
Any G	$ G $	$ G $	1	Point
C_k	k	k	1	Point
		1	k	Regular k -gons
D_2	4	2	2	Line
		1	4	Regular tetrahedron, infinitely many spheroids, infinitely many rectangles
D_ℓ	2ℓ	ℓ	2	Line
		2	ℓ	Regular ℓ -gon
		1	2ℓ	Infinitely many polyhedra
T	12	3	4	Regular tetrahedron
		2	6	Regular octahedron
		1	12	Infinitely many polyhedra
O	24	4	6	Regular octahedron
		3	8	Cube
		2	12	Cuboctahedron
		1	24	Infinitely many polyhedra
I	60	5	12	Regular icosahedron
		3	20	Regular dodecahedron
		2	30	Icosidodecahedron
		1	60	Infinitely many polyhedra

To let the robots agree on the total ordering among the elements of the $\gamma(P)$ -decomposition of P , the authors introduced the “local view” of each robot, which is determined by P independently of the local coordinate systems so that each robot r_i can compute the local view of $r_j \in R$ although r_i observes P in its local coordinate system Z_i . We will briefly describe how the robots compute local views. The local view of robot $r_i \in R$ is constructed by considering the innermost empty ball $I(P)$ as the earth and line $\overline{p_i b(P)}$ as the earth’s axis, where p_i is the position of r_i . Then the positions of each robot is represented by its amplitude, longitude, and latitude. To determine the meridian, r_i selects a robot nearest to $I(P)$ whose projection on $I(P)$ determines the meridian. If there are multiple candidates for a meridian robot, r_i selects one of them that minimizes r_i ’s local view, which is defined as follows: The local view of r_i is an n -tuple of positions of robots where the first element is the position of r_i , the second element is the position of the meridian robot, and the positions of the remaining robots are sorted in the increasing order. Because all local coordinate systems are right-handed, each robot can compute the local view of all robots. Then the robots agree on the lexicographic order of local view that guarantees the following properties: For a set of points P and its $\gamma(P)$ -decomposition $\{P_1, P_2, \dots, P_m\}$,

1. All robots in P_i have the same local view for each $i = 1, 2, \dots, m$.
2. Any two robots, one in P_i and the other in P_j , have different local views for all $i \neq j$.

The robots agree on a total ordering among the elements of the $\gamma(P)$ -decomposition of P by the ordering among local views so that the ordering satisfies the following properties.

Property 2. Let $P \in \mathcal{P}_n^3$ and $\{P_1, P_2, \dots, P_m\}$ be a configuration of robots recognized as a set of points and its $\gamma(P)$ -decomposition of P . Then, the local view defined in [21] guarantees the following properties:

1. P_1 is on $I(P)$ and P_m is on $B(P)$.

2. For each P_i and P_{i+1} , all points in P_{i+1} are on or in the exterior of $Ball(P_i)$.

Finally, we consider a decomposition of a set of points P by a rotation group $G \preceq \gamma(P)$. Given an embedding of G into $\gamma(P)$, we consider the orbit of G through each element $p \in P$ and the orbit space $\{Orb(p) : p \in P\} = \{P_1, P_2, \dots, P_\ell\}$. Clearly, $\{P_1, P_2, \dots, P_\ell\}$ is a partition of P and each subset in the family is a transitive set of points regarding G . We call this decomposition the G -decomposition of P . We will use such decomposition when we discuss impossibility in Section 3.4.

3.2 Rotation group of local coordinate systems

We introduce the rotation group of local coordinate systems of robots. Of course each robot recognizes neither the local coordinate systems of other robots nor the rotation group of them by just observing the positions of the robots. We use this notion when we discuss impossibility.

We denote an arrangement of local coordinate systems by a set of four-tuples $Q = \{(p_i, x_i, y_i, z_i) : r_i \in R\}$ where p_i represents the position of $r_i \in R$ in Z_0 and x_i, y_i, z_i are the positions $(1, 0, 0)$, $(0, 1, 0)$, and $(0, 0, 1)$ of Z_i observed in Z_0 . An arrangement of local coordinate systems encodes the positions of the robots since the current position of the robot is the origin of its local coordinate system. We also use the set of points $P = \{p_1, p_2, \dots, p_n\}$ to denote the positions of robots of Q .

We consider rotations on Q that produces the same arrangement of local coordinate systems.

Definition 2. *Let Q be a set of local coordinate systems of robots. The rotation group $\sigma(Q)$ of Q is the rotation group in \mathbb{S} that acts on Q and none of its proper supergroup in \mathbb{S} acts on Q .*

Clearly, $\sigma(Q)$ is uniquely determined for any set of local coordinate systems Q and it also determines the arrangement of rotation axes of $\sigma(Q)$ in Q that decomposes Q into disjoint subsets by the group action of $\sigma(Q)$. We call this decomposition $\sigma(Q)$ -decomposition of Q . We focus on the decomposition of P by $\sigma(Q)$ rather than the decomposition of Q by $\sigma(Q)$. When it is clear from the context, we denote $\sigma(Q)$ by $\sigma(P)$ and the $\sigma(Q)$ -decomposition of Q by $\sigma(P)$ -decomposition of P .

Clearly we have the following property.

Property 3. Let $P \in \mathcal{P}_n^3$ and $\{P_1, P_2, \dots, P_\ell\}$ be a configuration of robots recognized as set of points and its $\sigma(P)$ -decomposition. For each P_i ($1 \leq i \leq \ell$), the robot forming P_i have the same local observation.

We show several relation between $\gamma(P)$ and $\sigma(P)$. The following property is clear from the definition.

Property 4. Let $Q = \{(p_i, x_i, y_i, z_i) : r_i \in R\}$ and $P = \{p_i : r_i \in R\}$ be an arbitrary set of n local coordinate systems and the set of n positions of robots where p_i is the position of $r_i \in R$. Then we have $\sigma(P)(= \sigma(Q)) \preceq \gamma(P)$, thus there is an embedding of $\sigma(P)$ to $\gamma(P)$.

If a k -fold axis of $\sigma(P)$ contains a point of P , there should be $(k - 1)$ other robots on that point so that we can apply rotations around the axis. When P is a set of points, it does not contain such multiplicity.

Property 5. Let $P \in \mathcal{P}_n^3$ and $\{P_1, P_2, \dots, P_\ell\}$ be a configuration of robots recognized as a set of points and its $\sigma(P)$ -decomposition, respectively. Then, we have $|P_i| = |\sigma(P)|$ for each $1 \leq i \leq \ell$.

3.3 Rotation group of a multiset of points

Though the initial configuration and the target pattern contain no multiplicity, when we prove impossibility, we should consider executions of any arbitrary pattern formation algorithm that may generate multiplicity. In this section, we extend the rotation group and the symmetricity to a multiset of points.

Let $P \in \mathcal{P}_n^3$ be a multiset of n points. Intuitively, the rotation group $\gamma(P)$ of P and the rotation group $\sigma(P)$ of local coordinate systems of P are straightforward generalization of those for a set of points. We consider rotations that keep the positions and multiplicities of P .⁸

Definition 3. *Let $P \in \mathcal{P}_n^3$ be a multiset of points. The rotation group $\gamma(P)$ of P is the rotation group in \mathbb{S} that acts on P and none of its proper supergroup in \mathbb{S} acts on P .*

Definition 4. *Let Q be a multiset of local coordinate systems. The rotation group $\sigma(Q)$ of Q is the rotation group \mathbb{S} that acts on Q and none of its proper supergroup in \mathbb{S} acts on Q .*

Clearly, we have Lemma 3 and Lemma 4 for the rotation group of multiset of points.

We will show the first impossibility result. In the following, for a configuration of robots recognized as a (multi-)set of points P , we use the robot $r_i \in R$ and its position $p_i \in P$ interchangeably.

Lemma 2. *Let $P \in \mathcal{P}_n^3$ be an arbitrary initial configuration of oblivious FSYNC robots. For an arbitrary deterministic algorithm ψ and its execution $P(0)(= P), P(1), P(2), \dots$, we have $\sigma(P(t)) \succeq \sigma(P)$ for any $t \geq 0$, thus $\gamma(P(t)) \succeq \sigma(P)$.*

Proof. Let P and $\{P_1, P_2, \dots, P_\ell\}$ be an initial configuration and its $\sigma(P)$ -decomposition of P . We consider an execution $P(0)(= P), P(1), P(2), \dots$ of an arbitrary algorithm ψ . We focus on an arbitrary element P_i and $p_j \in P_i$. Because P is a set of n points, from Property 5, for any $p_k \in P_i$, there exists an element $g_k \in \sigma(P)$ that satisfies $g_k * p_j = p_k$ and $g_k \neq g_{k'}$ if $p_k \neq p_{k'}$. We will show that the movement of each $p_k \in P_i$ is symmetric regarding $\sigma(P)$ and the robots of P_i keep the rotation axes of $\sigma(P)$ in $P(1)$.

Consider the Compute phase at time 0 and let $\psi(Z_j(P(0))) = d_j$ at p_j . From Property 3, each robot $p_k \in P_i$ have the same local observation and $\psi(Z_k(P(0))) = \psi(Z_j(P(0))) = d_j$ at p_k . Because $p_k = g_k * p_j$, $Z_0(\psi(Z_k(p(0)))) = g_k * Z_0(\psi(Z_j(P(0))))$ and after the movement the positions of robots that formed P_i are symmetric regarding the same arrangement of $\sigma(P)$. Additionally, the local coordinate system of these robots are still symmetric regarding the same arrangement of $\sigma(P)$. Let $P_i(1) \subseteq P(1)$ be the positions of robots that formed P_i in $P(0)$. Hence, we have $\sigma(P_i(1)) = \sigma(P(0))$. Because this property holds for all P_i ($1 \leq i \leq \ell$), we have $\sigma(P(1)) \succeq \sigma(P(0))$. Note that $P(1)$ can be a multiset of points.

By repeating the above discussion, we can show that $\sigma(P(t)) \succeq \sigma(P(0))$ for any $t \geq 1$, thus $\gamma(P(t)) \succeq \sigma(P(0))$ for any $t \geq 1$. \square

We now consider the non-oblivious version of Lemma 2.

Lemma 3. *Let $P \in \mathcal{P}_n^3$ be an arbitrary initial configuration of non-oblivious FSYNC robots. For an arbitrary deterministic algorithm ψ and its execution $P(0)(= P), P(1), P(2), \dots$, we have $\sigma(P(t)) \succeq \sigma(P)$ for any $t \geq 0$, thus $\gamma(P(t)) \succeq \sigma(P)$.*

⁸ We do not define the decomposition of a multiset of points P by $\gamma(P)$ or $\sigma(P)$ in this section, but we need careful treatment as shown in Section 7. Additionally, the robots cannot agree on the ordering of the elements of the $\gamma(P)$ -decomposition of P since the second condition of Property 2 does not always hold because of multiplicities.

Proof. Let P and $\{P_1, P_2, \dots, P_\ell\}$ be an initial configuration where the content of local memory at all robots are identical and the $\sigma(P)$ -decomposition of P , respectively. Let $P(0)(= P), P(1), P(2), \dots$ be an execution of an arbitrary algorithm ψ . In the same way as the proof of Lemma 2, the robots forming each P_i ($i \in \{1, 2, \dots, \ell\}$) obtain the same local observation and same output of a common algorithm in $P(0)$, and their next positions keep the same arrangement of $\sigma(P)$. Hence in $P(1)$, their memory contents remain identical and these robots obtain the same local observation, and same output of a common algorithm. By repeating this discussion, robots can never break $\sigma(P)$ in any $P(t)$ ($t \geq 0$). \square

3.4 Symmetricity of a set of points

We start with the following observation. Consider a set of points P that forms a cube, thus $\gamma(P) = O$. We can embed D_4 to $\gamma(P)$ by selecting one 4-fold axis of $\gamma(P)$ as the principal axis and the other two 4-fold axes of $\gamma(P)$ as the secondary axes. The remaining two secondary axes overlap the 2-fold axes of $\gamma(P)$. The D_4 -decomposition of P consists of two elements and we construct an arrangement of local coordinate systems of robots so that $\sigma(P) = D_4$ by selecting one point p for each element of the D_4 -decomposition of P , fixing its local coordinate system, and applying the rotations of D_4 to p 's local coordinate system. From Lemma 2, the robots cannot reduce their rotation group to any subgroup of D_4 from such initial arrangement of local coordinate systems. Consequently, robots cannot eliminate an arbitrary rotation group $G \preceq \gamma(P)$ that produces $|G|$ symmetric local coordinate systems regarding G . Based on this observation, we define the *symmetricity* of a configuration as follows.

Definition 5. Let $P \in \mathcal{P}_n^3$ be a set of points. The symmetricity $\varrho(P)$ of P is the set of rotation groups $G \in \mathbb{S}$ that acts on P and there exists an embedding of G to $\gamma(P)$ such that each element of G -decomposition of P is a $|G|$ -set.

We define $\varrho(P)$ as a set because the ‘‘maximal’’ rotation group that satisfies the definition is not uniquely determined. Maximality means that there is no proper supergroup in \mathbb{S} that satisfies the condition of Definition 5. When it is clear from the context, we denote $\varrho(P)$ by the set of such maximal elements. For example, if P forms a regular icosahedron, $\varrho(P) = \{C_1, C_2, C_3, D_2, D_3, T\}$ and we denote it by $\varrho(P) = \{D_3, T\}$. (See Figure 4.) From the definition, $\varrho(P)$ always contains C_1 and if $G \in \varrho(P)$, $\varrho(P)$ contains every element of \mathbb{S} that is a subgroup of G .

Because $G \in \varrho(P)$ acts on P , G is a subgroup of $\gamma(P)$ and any initial configuration P is a set of n points, we can rephrase the above definition as follows: For an initial configuration P , $\varrho(P)$ is the set of rotation groups $G \in \mathbb{S}$ that has an embedding to unoccupied rotation axes of $\gamma(P)$ and if all rotation axes of $\gamma(P)$ is occupied, $\varrho(P) = \{C_1\}$.

From Lemma 2, we will show that for any $G \in \varrho(P)$, there exists an arrangement of local coordinate systems of P that satisfies $\sigma(P) = G$ and does not allow the robots to reduce their rotation group to a subgroup of G .

Lemma 4. Let P be an arbitrary initial configuration of oblivious FSYNC robots. For each $G \in \varrho(P)$, there exists an arrangement of local coordinate systems of P such that for an arbitrary algorithm and its execution $P(0)(= P), P(1), P(2), \dots, \gamma(P(t)) \succeq G$ for all $t \geq 0$.

Proof. From the definition, there exists an embedding of G to the unoccupied rotation axes of $\gamma(P)$. We select one of such embeddings and construct an initial arrangement of local coordinate systems for $P(= P(0))$ that satisfies $\sigma(P) = G$: Let $\{P_1, P_2, \dots, P_\ell\}$ be the G -decomposition of P

for the embedding of G . For each element P_i ($i = 1, 2, \dots, \ell$), we choose a point $p \in P_i$ and its local coordinate system, then apply the rotations of G . We obtain an arrangement of local coordinate systems with $\sigma(P) = G$.

From Lemma 2, for any execution $P(0)(= P), P(1), P(2), \dots$ of an arbitrary algorithm, $\gamma(P(t)) \succeq G$ for all $t \geq 0$. \square

In the same way as Lemma 3, local memory at robots does not help the robots break the symmetricity. Hence we have the following non-oblivious version of Lemma 4.

Lemma 5. *Let P be an arbitrary initial configuration of non-oblivious FSYNC robots. For each $G \in \varrho(P)$, there exists an arrangement of local coordinate systems of P such that for an arbitrary algorithm and its execution $P(0)(= P), P(1), P(2), \dots$, $\gamma(P(t)) \succeq G$ for all $t \geq 0$.*

4 Algorithm to show $\varrho(P)$

As shown in Section 3.3, the symmetricity of an initial configuration P consists of the rotation groups that the robots can never break. However there exists an initial configuration P such that $\varrho(P)$ does not contain $\gamma(P)$. For example, when P forms a cube, $\gamma(P) = O$ while $\varrho(P) = \{D_4\}$. In this case, there seems to be a possibility that the robots can reduce the symmetry of their positions. In this section, we will show that the robots can reduce symmetry of their positions and agree on some rotation group $G \in \varrho(P)$ with a very simple algorithm.

In 2D-space, the robots can reduce symmetry of their positions only when there is a robot on the center of the smallest enclosing circle of their positions, i.e., on the single rotation axis of their cyclic group. We will show that in 3D-space, in the same way, robots can reduce the rotation group of their positions by leaving rotation axes. For example, consider a configuration P where robots form a regular pyramid. Hence $\gamma(P) = C_k$ if the base is a regular k -gon. If the robot at the apex leaves the single rotation axis, the rotation group of the new configuration is C_1 that matches the symmetricity of the initial configuration. We will show such simple movement reduces the rotation group of the configuration.

Lemma 6. *There exists an algorithm ψ_{SYM} for oblivious FSYNC robots that translates an arbitrary initial configuration P to a configuration P' that satisfies $\gamma(P') \in \varrho(P)$.*

The proposed algorithm is based on the “go-to-center” algorithm in [21], that considers symmetry breaking in an initial configuration P whose $\gamma(P)$ -decomposition contains a regular tetrahedron, regular octahedron, a cube, a regular dodecahedron, or an icosidodecahedron. When the robots form these polyhedra, they are on some rotation axes of $\gamma(P)$ and the “go-to-center” algorithm sends the robots to some point not on any rotation axis. Because the number of robots is less than $|\gamma(P)|$, the positions of robots are not transitive regarding $\gamma(P)$ and the rotation group of any resulting configuration is no more $\gamma(P)$. We apply the “go-to-center” algorithm to all configurations where some rotation axes of $\gamma(P)$ are occupied. Specifically, we add a cuboctahedron and a regular icosahedron to the target of the algorithm and analyze the rotation group of resulting configurations. We also add similar symmetry breaking procedures for configurations with a 2D rotation group. We will show that as is expected from the results in 2D-space, when some rotation axes of $\gamma(P)$ are occupied, the robots on the rotation axes can remove the rotation axes by leaving their current positions, thus the symmetricity of a resulting configuration is a proper subgroup of the rotation group of the previous configuration. By repeating this procedure, the robot system reaches a configuration P' with $\gamma(P') \in \varrho(P)$. We first analyze the configuration after one-step execution of the

Table 3. Symmetricity of $U_{G,\mu} \cup U_{G,1}$.

Rotation group	Folding	Polyhedra formed by $U_{G,\mu}$	Notation	$\varrho(U_{G,1} \cup U_{G,\mu})$
Any $G \in \mathbb{S}$	$ G $	Point at the center	$U_{G, G }$	$\{C_1\}$
C_k	k	Point on the single rotation axis	$U_{C_k,k}$	$\{C_1\}$
	1	Regular k -gon	$U_{C_k,1}$	$\{C_k\}$
D_2	2	Line on a rotation axis	$U_{D_2,2}$	$\{C_2\}$
	1	Regular tetrahedron, infinitely many sphenoids, and infinitely many rectangles	$U_{D_2,1}$	$\{D_2\}$
D_ℓ	ℓ	Line on the principal axis	$U_{D_\ell,\ell}$	$\{C_2\}$
	2	Regular ℓ -gon perpendicular to the principal axis and containing the center	$U_{D_\ell,2}$	$\{C_\ell, D_{\ell/2}\}$ if ℓ is even, $\{C_\ell\}$ otherwise
	1	Infinitely many polyhedra	$U_{D_\ell,1}$	$\{D_\ell\}$
T	3	Regular tetrahedron	$U_{T,3}$	$\{D_2\}$
	2	Regular octahedron	$U_{T,2}$	$\{D_3\}$
	1	Infinitely many polyhedra	$U_{T,1}$	$\{T\}$
O	4	Regular octahedron	$U_{O,4}$	$\{D_3\}$
	3	Cube	$U_{O,3}$	$\{D_4\}$
	2	Cuboctahedron	$U_{O,2}$	$\{T, C_4, C_3\}$
	1	Infinitely many polyhedra	$U_{O,1}$	$\{O\}$
I	5	Regular icosahedron	$U_{I,5}$	$\{T, D_3\}$
	3	Regular dodecahedron	$U_{I,3}$	$\{D_5, D_2\}$
	2	Icosidodecahedron	$U_{I,2}$	$\{C_5, C_3\}$
	1	Infinitely many polyhedra	$U_{I,1}$	$\{I\}$

“go-to-center” algorithm when the robots form one of the above seven (semi-)regular polyhedra in Section 4.1 and then we consider any initial configuration where some of its rotation axes are occupied in Section 4.2.

Let $\{P_1, P_2, \dots, P_m\}$ be the $\gamma(P)$ -decomposition of an initial configuration P . We focus on the elements that consist of points on rotation axes of $\gamma(P)$. In other words, we focus not on the coordinates of each point but on $\gamma(P)$ and the folding of each element of its $\gamma(P)$ -decomposition. We denote a polyhedron generated by a rotation group G and a seed point s with folding μ as $U_{G,\mu}$. Table 3 shows the list of $U_{G,\mu}$ for $G \in \mathbb{S}$ and the symmetricity of $U_{G,\mu} \cup U_{G,1}$ as an example. For example, a configuration $U_{O,1} \cup U_{O,3}$ consists of a truncated cube and a cube with a common arrangement of O . We note that we need $U_{G,1}$ for the 2D rotation groups and when G is a 3D rotation group, $\varrho(U_{G,\mu})$ and $\varrho(U_{G,1} \cup U_{G,\mu})$ are identical.

We first note that there is no way for oblivious FSYNC robots to reduce $\gamma(P)$ of an initial configuration P when P forms a regular n -gon. Here, $\gamma(P) = D_n$ and $\varrho(P) = \{C_n, D_{n/2}\}$ if n is even, $\varrho(P) = \{C_n\}$ otherwise. Consider the case where n is even. To show the symmetricity, the robots either show an orientation of the single rotation axis or divide themselves into two groups to form $U_{D_{n/2},1}$. However, when $\sigma(P) = C_n$, from Lemma 4, the rotation group of robots is C_n forever, thus they keep some regular n -gon forever. The robots neither show an agreement on the orientation of the principal axis nor divide themselves into two groups. When the robots are oblivious, they do not remember the previous trials without recognizing $\sigma(P) = C_n$ and they keep on trying to show their symmetricity forever. We have the same situation for odd n . We avoid this infinite trials by leaving a regular n -gon as it is. Hence the proposed algorithm do nothing when P

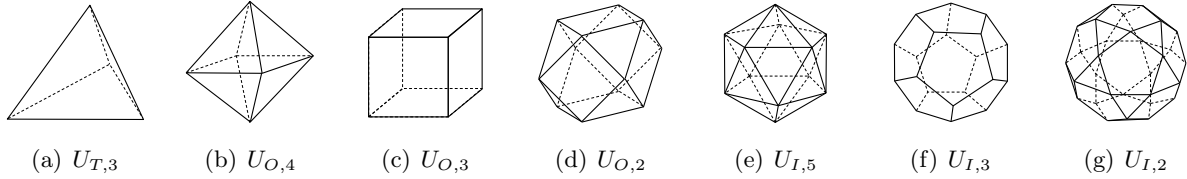


Fig. 6. Seven polyhedra

Algorithm 4.1 Go-to-center(P) for robot $r_i \in R$

Notation

- P : The positions of robots forming an $U_{G,\mu}$ for $G \in \{T, O, I\}$ and $\mu > 1$ observed in Z_i .
- p_i : Current position of r_i .
- ϵ : $\ell/100$ where ℓ is the length of an edge of the polyhedron that P forms.

Algorithm

Switch (P) **do**

Case cuboctahedron:

 Select an adjacent triangle face.

 Destination d is the point ϵ before the center of the selected face on the line from p_i to the center.

Case icosidodecahedron:

 Select an adjacent pentagon face.

 Destination d is the point ϵ before the center of the selected face on the line from p_i to the center.

Default:

 Select an adjacent face.

 Destination d is the point ϵ before the center of the selected face on the line from p_i to the center.

Enddo

forms a regular polygon. This is not a problem for Theorem 1 since for such P , the target pattern F satisfies $C_n, D_{n/2} \in \varrho(F)$ and hence $\gamma(F) \succeq D_n$ and the robots do not need to break the symmetry.

4.1 Transitive set of points

We start with a symmetry breaking algorithm for a transitive initial configuration regarding a 3D rotation group, i.e., we consider $U_{G,\mu}$ for $G \in \{T, O, I\}$ and $\mu > 1$, a regular tetrahedron, a regular octahedron, a cube, a cuboctahedron, a regular icosahedron, a regular dodecahedron, and an icosidodecahedron (Figure 6). The proposed algorithm is based on the “go-to-center” algorithm of [21] as shown in Algorithm 4.1. If a current configuration forms one of the above seven polyhedra, Algorithm 4.1 makes each robot select an adjacent face and approach the center of the selected face, but stops it ϵ before the center. There are two restrictions, i.e., when the robots form a cuboctahedron or an icosidodecahedron, they select one face from adjacent regular triangle faces or adjacent regular pentagon faces, respectively. The aim of the algorithm is to put the robots on some points that are not on any rotation axis. The role of ϵ is to gather the robots around some rotation axis and we fix ϵ to $\ell/100$ for the simplicity of the proposed algorithm where ℓ is the length of an edge of the (semi-)regular polyhedron that the robots initially form.

Lemma 7. *Let P be an arbitrary initial configuration of oblivious FSYNC robots that forms a $U_{G,\mu}$ for $G \in \{T, O, I\}$ and $\mu > 1$. One step execution of Algorithm 4.1 translates P to another configuration P' that satisfies $\gamma(P') \in \varrho(P)$.*

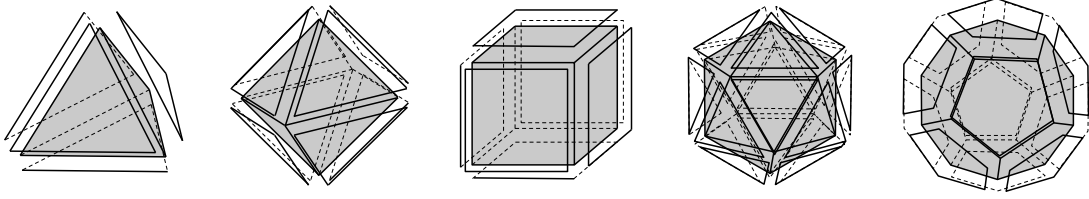


Fig. 7. Expansion of base polyhedra.

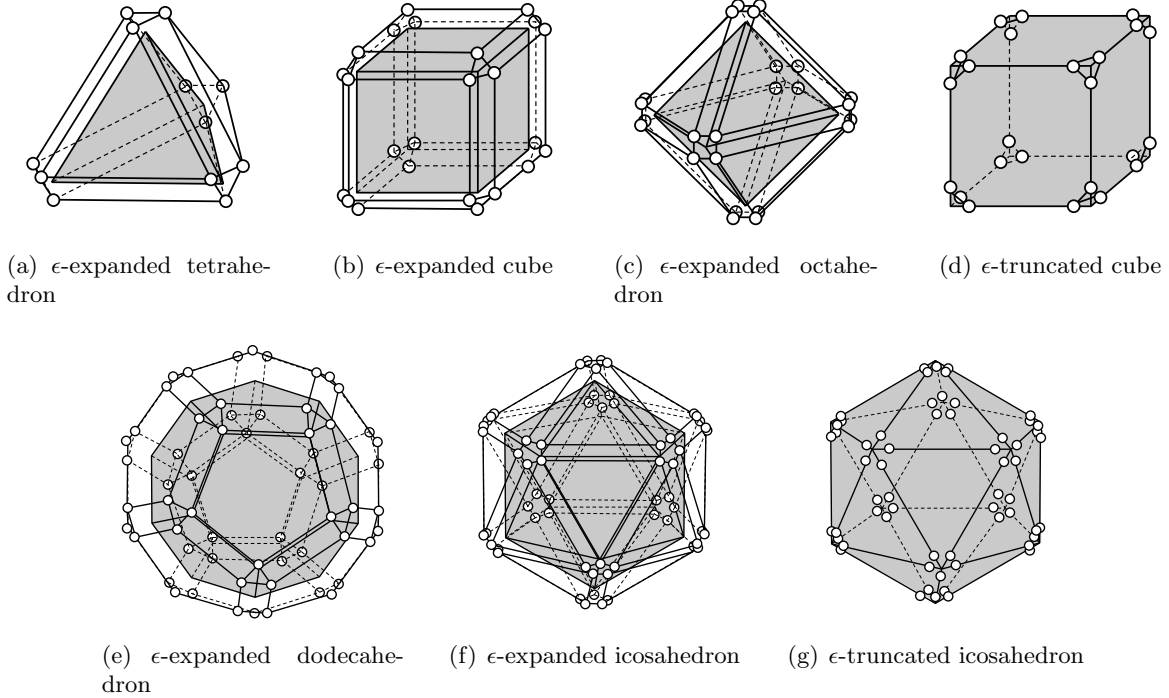


Fig. 8. Candidate set D corresponding to P .

Proof. Let P, P' be an initial configuration that forms one of the above seven (semi-)regular polyhedra and a configuration obtained by one-step execution of Algorithm 4.1. We will show that $\gamma(P') \in \varrho(P)$.

The proof follows the same idea as [21]. Let D be the set of all points that can be selected by the robots as their next positions in P . When P is a regular polyhedron, the points of D are placed around the vertices of the dual of P , which we call the *base polyhedron* for D . For example, when P is a cube, the base polyhedron is a regular octahedron (Figure 8(c)). When P is a cuboctahedron (an icosidodecahedron, respectively), the next positions are placed around the 3-fold axes of O (the 5-fold axes of I , respectively). In this case, we consider a cube (a regular icosahedron, respectively) as its base polyhedron.

Figure 8 shows the base polyhedron and the set of possible destinations D for each of the seven initial configurations. When P is a regular polyhedron, D forms a polyhedron obtained by moving each face of the base polyhedron away from the center with keeping the center. Then the obtained

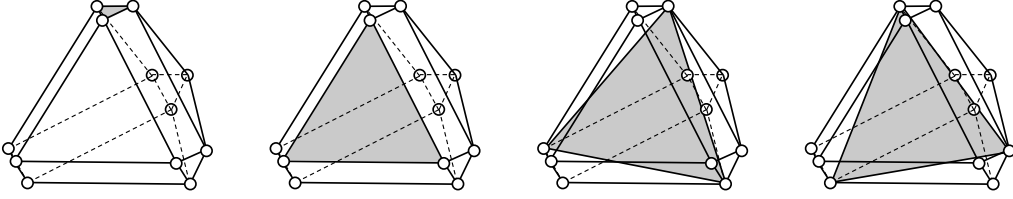


Fig. 9. Regular triangles in an ϵ -expanded tetrahedron.

polyhedron consists of the faces of the base polyhedron and new faces formed by the separated vertices and the separated edges of the base polyhedron.⁹ See Figure 7. For example, when P is a cube, D forms a polyhedron obtained by a regular octahedron with the above operation and we call the polyhedron ϵ -expanded octahedron (Figure 8(c)). In the same way, if P is a regular tetrahedron, D forms an ϵ -expanded tetrahedron (Figure 8(a)), if P is a regular octahedron, D forms an ϵ -expanded cube (Figure 8(b)), if P is a regular icosahedron, D forms an ϵ -expanded dodecahedron (Figure 8(e)), and if P is a regular dodecahedron, D forms an ϵ -expanded icosahedron (Figure 8(f)). On the other hand, when P is a semi-regular polyhedron, D forms a polyhedron obtained by cutting the vertices of the base polyhedron. For example, when P is a cuboctahedron, D is a polyhedron obtained from a cube by cutting its vertices and we call the polyhedron an ϵ -truncated cube (Figure 8(d)). If P is a icosidodecahedron, D forms an ϵ -truncated icosahedron (Figure 8(g)). It is worth emphasizing that D is a transitive set of points regarding $\gamma(P)$, thus it is spherical.

Algorithm 4.1 makes the robots select a subset of size $|P|$ from D . To prove the correctness, we will show that the symmetricity of any such subset has the rotation group that satisfies the statement.

Our basic idea is to check all possibilities of $\gamma(P')$, specifically, for each $G \notin \varrho(P)$, we assume that $\gamma(P') = G$ and check the $\gamma(P')$ -decomposition of P' . From Algorithm 4.1, any resulting configuration P' contains multiplicity since the sets of possible next positions of different robots are disjoint.

Case A. P is a regular tetrahedron: D forms an ϵ -expanded tetrahedron and we check the rotation group of any 4-set of D . We will show $\gamma(P') \in \varrho(P) = \{D_2\}$.

Assume that $\gamma(P')$ is D_k or C_k for some $k \geq 3$. Because we cannot find any regular ℓ -gon for $\ell \geq 4$ in D , $k \leq 3$.

Assume $\gamma(P') = D_3$, then the D_3 -decomposition of P' consists of $U_{D_3,2}$ (cardinality 3) and $U_{D_3,6}$ (cardinality 1) because P' consists of four points. We do not have the case where the D_3 -decomposition of P' consists of two $U_{D_3,3}$'s (i.e., all points of P' are on the principal axis of D_3), because $\gamma(P') = D_\infty$. Thus P' contains a regular triangle. Figure 9 shows all possible regular triangles in an ϵ -expanded tetrahedron and we cannot find any regular triangle that have one point of D at its center. Hence $\gamma(P') \neq D_3$.

Assume $\gamma(P') = C_3$, then the C_3 -decomposition of P' consists of $U_{C_3,1}$ (cardinality 3) and $U_{C_3,3}$ (cardinality 1), because otherwise $\gamma(P')$ is not C_3 . Thus P' contains a regular triangle. In the same way, for any regular triangle in D , there is no point on the 3-fold axis for the triangle. Hence $\gamma(P') \neq C_3$. Consequently, if $\gamma(P')$ is a 2D rotation group, it is C_1 , C_2 , or D_2 .

⁹ The operation is also known as *cantellation*: the convex hull of D is obtained from the base polyhedron by truncating the vertices and beveling the edges. See [4].

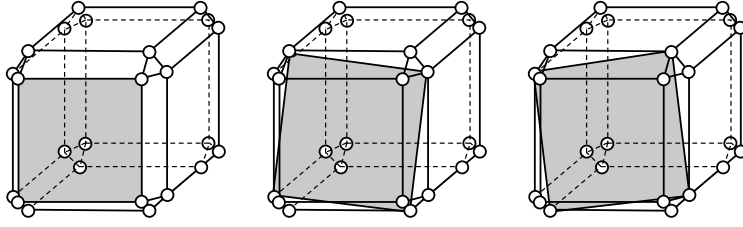


Fig. 10. Square in an ϵ -expanded cube.

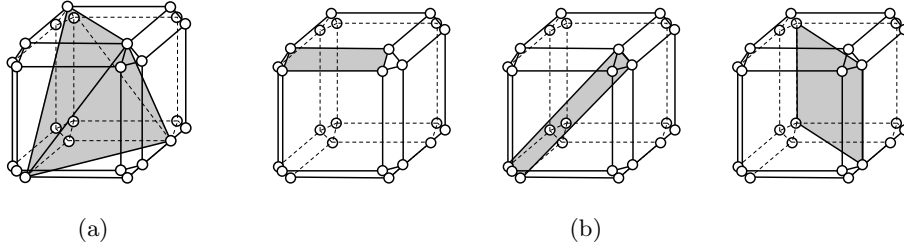


Fig. 11. An example of $U_{D_{2,1}}$ in an ϵ -expanded cube. (a) A sphenoid. (b) A rectangle.

We check the 3D rotation groups. First, $\gamma(P') \neq T$ since any polyhedron with rotation group T consists of more than four points and there is no 4-set that forms a regular tetrahedron (i.e., the base polyhedron) in an ϵ -expanded tetrahedron. Second, $\gamma(P')$ is neither O nor I since any polyhedron with rotation group O (or I) consists of at least 6 (12, respectively) vertices. (See Table 2.)

Consequently, $\gamma(P') \preceq D_2$.

Case B. P is a regular octahedron: D forms an ϵ -expanded cube and we check the rotation group of any 6-set of D . We will show $\gamma(P') \in \varrho(P) = \{D_3\}$.

Assume that $\gamma(P)$ is D_k or C_k for some $k \geq 4$. Because we cannot find any regular ℓ -gon for $\ell \geq 5$ in D , $k \leq 4$.

Assume $\gamma(P') = D_4$, then the D_4 -decomposition of P' consists of $U_{D_{4,2}}$ (cardinality 4) and $U_{D_{4,4}}$ (cardinality 2) because P' consists of six points. We do not have the case where D consists of three $U_{D_{4,4}}$'s since $P\gamma(P') = D_\infty$. Thus P' contains a square. Figure 10 shows all possible squares in an ϵ -expanded cube and we cannot find any square that have two points on its 4-fold axis. Hence $\gamma(P') \neq D_4$.

Assume $\gamma(P') = C_4$, then the C_4 -decomposition of P' consists of $U_{C_{4,1}}$ (cardinality 4) and two $U_{C_{4,4}}$'s (cardinality 1). Thus P' contains a square. In the same way, for any square in D , there is no point on the 4-fold axis for the square. Hence $\gamma(P') \neq C_4$.

Assume $\gamma(P') = D_2$, then the D_2 -decomposition of P' consists of (i) $U_{D_{2,1}}$ (cardinality 4) and $U_{D_{2,2}}$ (cardinality 2) or (ii) three $U_{D_{2,2}}$'s (cardinality 2). We first check case (i) where $U_{D_{2,1}}$ forms a sphenoid, a regular tetrahedron, a rectangle, or a square. See Figure 11 as an example. Now consider $\epsilon \rightarrow 0$. If $U_{D_{2,1}}$ forms a sphenoid or a regular tetrahedron, when $\epsilon = 0$, $U_{D_{2,1}}$ forms a regular tetrahedron in the base polyhedron. (See Figure 12(a).) However, there is no vertex of the base polyhedron on the 2-fold axes of the regular tetrahedron. When $\epsilon > 0$, the arrangement of

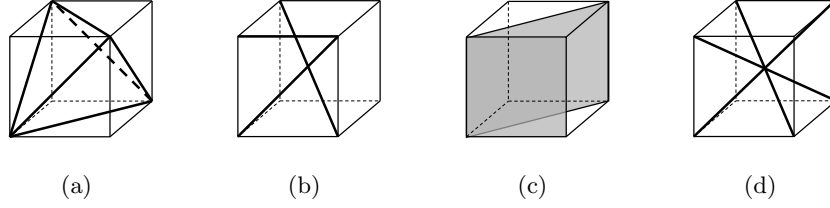


Fig. 12. Lines and rectangles of base polyhedron cube. (a) A regular tetrahedron in a cube. (b) We have two kinds of rectangles formed by four vertices of a cube. (c) Three lines intersecting one point in the cube are not perpendicular to each other.

edges of $U_{D_2,1}$ slightly moves from the regular tetrahedron, but we cannot find two points forming $U_{D_2,2}$ on the 2-fold axes of $U_{D_2,1}$.

In the same way, if $U_{D_2,1}$ forms a rectangle or a square, when $\epsilon = 0$, $U_{D_2,1}$ forms a line formed by two vertices of the base polyhedron or a rectangle formed by four vertices of the base polyhedron (See Figure 12(b) and Figure 12(c).) There are three possibilities for a line; edges of the base polyhedron, diagonals of the faces of the base polyhedron, or diagonals of the base polyhedron (connecting two opposite vertices). In any of the three cases, there is no pair of vertices of the base polyhedron that form a perpendicular bisector or a line on it. When $\epsilon > 0$, the arrangement of edges of $U_{D_2,1}$ slightly moves from the line, but we cannot find two points forming $U_{D_2,2}$ on the 2-fold axes of $U_{D_2,1}$. There are two possibilities for a square; faces of the base polyhedron or the rectangle cutting the base polyhedron into two triangular prisms. In both cases, there are no pair of vertices of the base polyhedron that are on some 2-fold axis or 4-fold axis of these rectangles. When $\epsilon > 0$, the arrangement of edges of $U_{D_2,1}$ slightly moves from the rectangles, but we cannot find two points forming $U_{D_2,2}$ on the 2-fold axes of $U_{D_2,1}$.

We check case (ii) where P' consists of three $U_{D_2,2}$'s. Because D is spherical, there is no three points of D that are on the same line. Hence the three $U_{D_2,2}$'s are perpendicular to each other and intersects at their midpoints, i.e., these three lines are in the interior of D . Consider $\epsilon \rightarrow 0$. When $\epsilon = 0$, three $U_{D_2,2}$'s degenerates to three lines formed by the vertices of the base polyhedron and perpendicular to each other. However we cannot find any three lines perpendicular to each other in a cube. (See Figure 12(d).) When $\epsilon > 0$, the arrangement of lines slightly moves from the rectangles, but we cannot find any three lines perpendicular to each other.

From case (i) and (ii), we have $\gamma(P') \neq D_2$.

We check the 3D rotation groups. First, assume $\gamma(P') = T$, then the T -decomposition of P' consists of $U_{T,2}$ since P' consists of 6 points. Because all points of D are near the vertices of a cube, P' does not form a regular octahedron (the dual of the base polyhedron). Hence $\gamma(P') \neq T$. Second, assume $\gamma(P') = O$, then the O -decomposition of P' consist of $U_{O,4}$, but as already discussed, we cannot find any regular octahedron in D . Finally, $\gamma(P') \neq I$ since any polyhedron with rotation group I consists of more than 12 vertices.

Consequently, $\gamma(P') \preceq D_3$.

Case C. P is a cube: D forms an ϵ -expanded octahedron and we check the rotation group of any 8-set of D . We will show $\gamma(P') \in \varrho(P) = \{D_4\}$.

Assume $\gamma(P')$ is D_k or C_k for some $k \geq 5$. Because we cannot find any regular ℓ -gon for $\ell \geq 5$ in D , $k \leq 4$.

Assume $\gamma(P') = D_3$, then the D_3 -decomposition of P' contains at least one $U_{D_3,3}$ (cardinality 2) or $U_{D_3,6}$ (cardinality 1) since $|P'| = 8$ is not divided by 3. Additionally, P' contains $U_{D_3,1}$

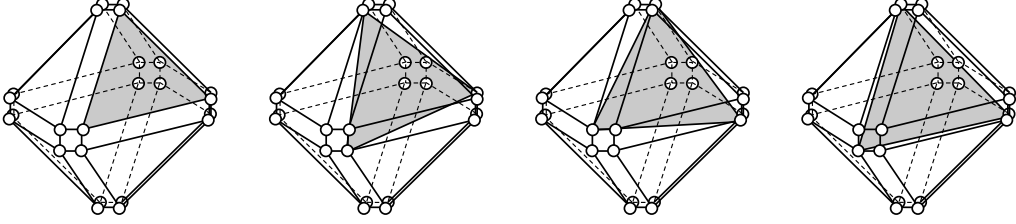


Fig. 13. Regular triangles in an ϵ -expanded octahedron.

(cardinality 6) or $U_{D_3,2}$ (cardinality 3), thus at least one regular triangle. Figure 13 shows all possible regular triangles in an ϵ -expanded octahedron and we cannot find any regular triangle that have a point on its 3-fold axis. Hence $\gamma(P') \neq D_3$.

Assume $\gamma(P') = C_3$, then the C_3 -decomposition of P' contains at least one $U_{C_3,3}$ (cardinality 1) since $|P'| = 8$. Additionally, P' contains $U_{C_3,1}$, thus at least one regular triangle. In the same way, for any regular triangle in D , there is no point on the 3-fold axis of the triangle. Hence $\gamma(P') \neq C_3$.

We check the 3D rotation groups. First, assume $\gamma(P') = T$, then the T -decomposition of P' consists of two $U_{T,3}$'s (cardinality 4) because P' consists of eight points. However, because the vertices of an ϵ -expanded octahedron is around the vertices of a regular octahedron, we cannot find any regular tetrahedron in D . Hence $\gamma(P') \neq T$.

Second, assume $\gamma(P') = O$, then the O -decomposition of P' consists of one $U_{O,3}$ (cardinality 8), but an ϵ -expanded octahedron does not contain any cube (its dual). Hence $\gamma(P') \neq O$.

Finally, $\gamma(P') \neq I$ since any polyhedron with rotation group I consists of at least 12 vertices (See Table 2).

Consequently, $\gamma(P') \preceq D_4$.

Case D. When P is a cuboctahedron: D forms an ϵ -truncated cube and we check the rotation group of any 12-set of D . We will show $\gamma(P') \in \varrho(P) = \{T, C_4, C_3\}$.

Assume that $\gamma(P')$ is C_k or D_k for some $k \geq 5$. Because we cannot find any regular ℓ -gon for $\ell \geq 5$ in D , $k \leq 4$.

Assume $\gamma(P') = D_4$, then the D_4 -decomposition of P' consists of (i) three $U_{D_4,2}$'s (cardinality 4), (ii) several $U_{D_4,4}$'s (cardinality 2) and $U_{D_4,2}$ or $U_{D_4,1}$ (cardinality 8) or (iii) one $U_{D_4,1}$ and one $U_{D_4,2}$ (cardinality 4). We do not have the case where we have six $U_{D_4,4}$'s since $\gamma(P') = D_\infty$. In any case, P' contains a square. Figure 14 shows all possible squares in an ϵ -truncated cube. We cannot find any three squares on a plane in D , hence we do not have case (i). Additionally, we cannot find any square in D that have points on its 4-rotation axis and we do not have case (ii). Now we consider case (iii) where P' contains a $U_{D_4,1}$ consisting of two squares shown in Figure 14. $U_{D_4,1}$ consists two congruent squares, thus they are on the same plane, or two congruent squares or they are opposite against the center of D . $U_{D_4,2}$ is on the 2-fold axis of D_4 , thus on the plane between the two bases, but we cannot find any point of D on such plane. Hence $\gamma(P') \neq D_4$.

Assume $\gamma(P') = D_3$, then the D_3 -decomposition of P' consists of (i) four $U_{D_3,2}$'s (cardinality 3), (ii) two $U_{D_3,1}$'s (cardinality 6), (iii) two $U_{D_3,2}$'s (cardinality 3) and $U_{D_3,1}$ (cardinality 6) or (iv) contains $U_{D_3,3}$ (cardinality 2). In any case, P' contains a regular triangle. Figure 15 shows all possible regular triangles in the ϵ -truncated cube. We first note that we cannot find any four regular triangles on the same plane, hence we do not have case (i). Next, consider case (iii). Two $U_{D_3,2}$'s are on the same plane and $U_{D_3,1}$ is symmetric against that plane. Find that any $U_{D_3,1}$ in

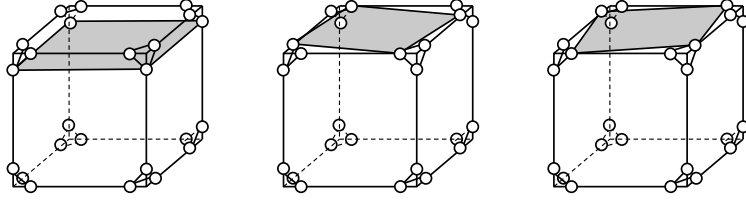


Fig. 14. Squares in an ϵ -truncated cube.

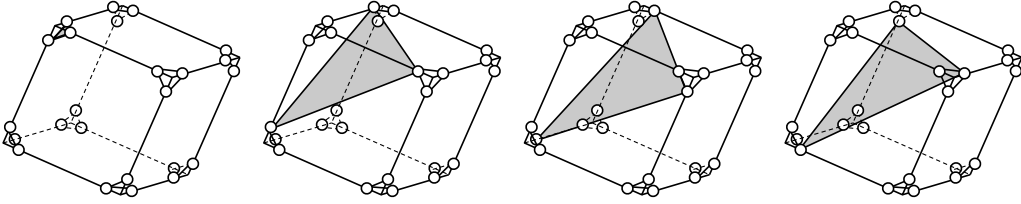


Fig. 15. Regular triangles in an ϵ -truncated cube.

D consists of opposite triangles against $b(D)$ that share the 3-fold axis of D . Hence there is no such two $U_{D_{3,2}}$'s in between the bases of $U_{D_{3,1}}$ and we do not have case (iii). We do not have case (iv) because there is no regular triangle that have some point of D on its 3-fold axis as shown in Figure 15.

Finally, we consider case (ii). The only possibility to form two $U_{D_{3,1}}$'s is to choose one base from the four triangles shown in Figure 15. We divide the long edges of the ϵ -truncated cube by a decomposition of the base polyhedron. We can cut a regular cube into two triangular pyramids and one triangular anti-prism. The first group consists of the edges of the ϵ -truncated cube contained in the two triangular prisms and the second group consists of the edges of the ϵ -truncated cube contained in the triangular anti-prism. (See Figure 16.) Remember that the two endpoints of each long edge of the ϵ -truncated cube are the destinations of one robot and P' contains just one of them. From the endpoints of the first group we can construct at most one triangular anti-prism (i.e., $U_{D_{3,1}}$). Then we check the endpoints of the second group and we can form two triangular anti-prisms each of which contains both endpoints of long edges of D since the arrangement of D_3 for the first group and that of the second group should be common. (See Figure 17.) Thus P' cannot contain two $U_{D_{3,1}}$'s and $\gamma(P') \neq D_3$.

We check the 3D rotation groups. First, assume $\gamma(P') = O$, then the O -decomposition of P' consists of two $U_{O,4}$'s (cardinality 6) or $U_{O,2}$ (cardinality 12) because $|P'| = 12$. Because the vertices of an ϵ -truncated cube is around the vertices of a regular cube, we can find neither any regular octahedron (i.e., its dual) in D nor any cuboctahedron in D .

Next, assume $\gamma(P') = I$, then the I -decomposition of P' consists forms $U_{I,5}$ (cardinality 12) because $|P'| = 12$. Because the vertices of an ϵ -truncated cube is around the vertices of a cube, we cannot find any regular icosahedron in D .

Consequently, $\gamma(P') \preceq C_4, C_3$, or T .

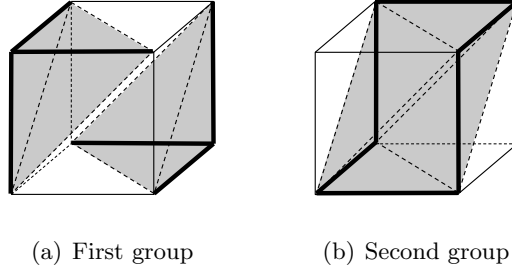


Fig. 16. Decomposition of the edges of an ϵ -truncated cube around a 3-fold axis by using the base polygon. The bold edges show the member edges of each group.

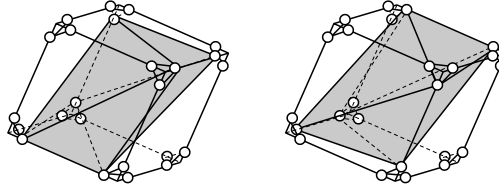


Fig. 17. $U_{D_{3,1}}$ in the second group of an ϵ -truncated cube.

Case E. P is a regular icosahedron: D forms an ϵ -expanded dodecahedron and we check the rotation group of any 12-set of D . We will show $\gamma(P') \in \varrho(P) = \{T, D_3\}$.

Assume that $\gamma(P')$ is D_k or C_k for some $k \geq 2$. Because we cannot find any regular ℓ -gon for $\ell \geq 6$ in D , $k \leq 5$.

Assume that $\gamma(P')$ is D_4 or C_4 , then P' contains at least one square. We would like to check all possible squares in D , but clearly any edge of an ϵ -expanded dodecahedron does not form any square because it does not have any adjacent edge with the same length and perpendicular to it. The remaining possibilities are the lines connecting the vertices of the ϵ -expanded dodecahedron. See Figure 18 that shows an embedding of a cube into a regular dodecahedron (the base polyhedron).¹⁰ Because the points of D are obtained by expanding the faces of a regular dodecahedron, there is no 4-set of D that forms a square. Hence $\gamma(P') \neq C_4, D_4$.

Assume that $\gamma(P')$ is D_5 or C_5 . Because $|P'|$ is not divided by 5, P' contains at least one $U_{D_5,5}$ (cardinality 2) or $U_{C_5,5}$ (cardinality 1). Figure 19 shows all possible regular pentagons in D and for each of the pentagons there is no vertex on its 5-fold axis. Hence $\gamma(P') \neq C_5, D_5$.

We check the 3D rotation groups. First, assume $\gamma(P') = O$, then the O -decomposition of P' consists of one $U_{O,2}$ (cardinality 12) or two $U_{O,4}$'s (cardinality 6) because $|P'| = 12$. Because the vertices of an ϵ -expanded dodecahedron is around the vertices of a regular dodecahedron, we can find neither a cuboctahedron nor regular octahedron in D .

Next, assume $\gamma(P') = I$, then the I -decomposition of P' consists of $U_{I,5}$ (cardinality 12) because $|P'| = 12$. Because the vertices of an ϵ -expanded dodecahedron is around the vertices of a regular dodecahedron, we cannot find any regular icosahedron (i.e., its dual) in D .

¹⁰ There are five such embeddings, but it is sufficient to check one of them because we just use it to check the arrangement of vertices.

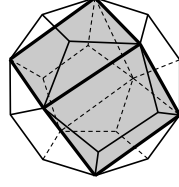


Fig. 18. A cube embedded in a regular dodecahedron.

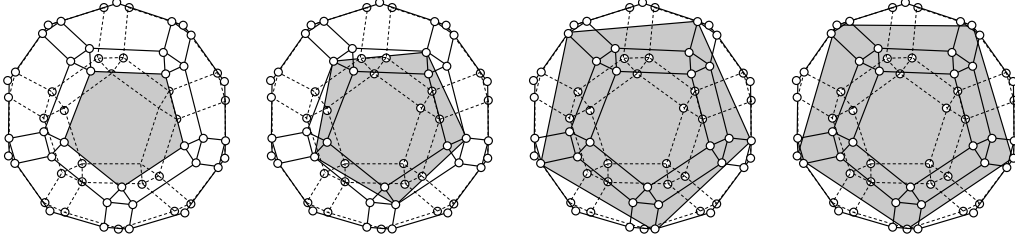


Fig. 19. Regular pentagons in an ϵ -expanded dodecahedron

Consequently, $\gamma(P') \preceq D_3$ or T .

Case F. P is a regular dodecahedron: D forms an ϵ -expanded icosahedron and we check the rotation group of any 20-set of D . We will show $\gamma(P') \in \varrho(P) = \{D_5, D_2\}$.

Assume that $\gamma(P')$ is D_k or C_k for some $k \geq 3$. Because we cannot find any regular ℓ -gon in D for $\ell = 4$ and $\ell \geq 6$, $k = 3$ or 5 .

Assume that $\gamma(P')$ is D_3 or C_3 . Because $|P'|$ is not divided by 3, P' contains at least one $U_{D_3,3}$ (cardinality 2) or $U_{C_3,1}$ (cardinality 1). Figure 20 shows all possible regular triangles in D and for each of the triangles there is no vertex on its 3-fold axis. Hence $\gamma(P') \neq C_3, D_3$.

We check the 3D rotation groups. First, assume $\gamma(P') = T$, then the T -decomposition of P' contains at least one $U_{T,3}$ (cardinality 4) or $U_{T,2}$ (cardinality 6) because $|P'| = 20$ is not divided by 12. Because the vertices of an ϵ -expanded icosahedron is around the vertices of a regular icosahedron, we can find neither a regular tetrahedron nor a regular octahedron in D . Hence $\gamma(P') \neq T$.

Second, assume $\gamma(P') = O$, then the O -decomposition of P' consists of two $U_{O,4}$'s (cardinality 6) and one $U_{O,3}$ (cardinality 8) because $|P'| = 20$. Because the vertices of an ϵ -expanded icosahedron is around the vertices of a regular icosahedron, we can find neither a cube nor a regular octahedron in D . Hence $\gamma(P') \neq O$.

Finally, assume $\gamma(P') = I$, then the I -decomposition of P' forms a $U_{I,3}$ (cardinality 20) because $|P'| = 20$. Because the vertices of an ϵ -expanded icosahedron is around the vertices of a regular icosahedron, we cannot find a regular dodecahedron (i.e., its dual) in D . Hence $\gamma(P') \neq I$.

Consequently, $\gamma(P') \preceq D_2$ or D_5 .

Case G. P is a icosidodecahedron: D forms an ϵ -truncated icosahedron and we check the rotation group of any 30-set of D . We will show $\gamma(P') \in \varrho(P) = \{C_5, C_3\}$.

Assume that $\gamma(P')$ is D_k or C_k for some $k \geq 2$. Because we cannot find any regular ℓ -gon in D for $\ell = 4, 6, 7, \dots$, $k = 2, 3$, or 5 .

Assume $\gamma(P') = D_2$, then the D_2 -decomposition of P' contains at least one $U_{D_2,2}$ (cardinality 2) because $|P'| = 30$ is not divided by 4. However, D_2 -decomposition of P' does not consist of only

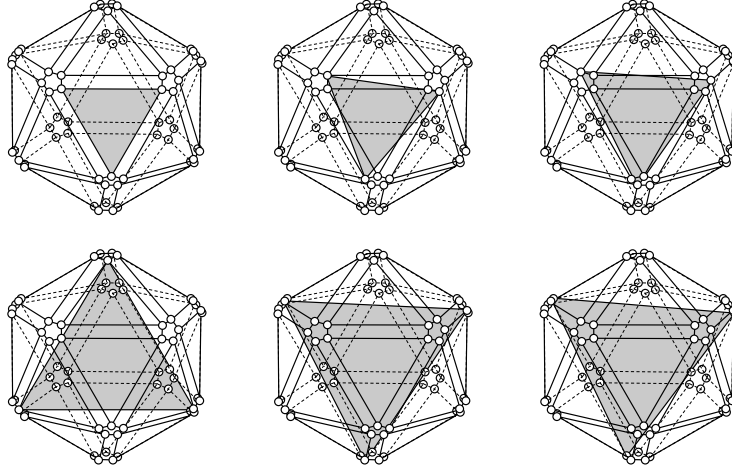


Fig. 20. Regular triangles in an ϵ -expanded icosahedron.

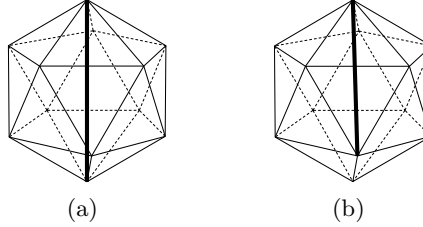


Fig. 21. Long edges in the interior of a regular icosahedron.

$U_{D_2,2}$'s, otherwise P' consists of 15 $U_{D_2,2}$'s and there is at least one 2-fold axes of D_2 that contains more than two $U_{D_2,2}$'s (i.e., 4 points). However, there is no line containing more than two points of D since D is spherical. Hence P' contains at least one $U_{D_2,1}$, i.e., a sphenoid, a regular tetrahedron, a rectangle, or a square. Now consider $\epsilon \rightarrow 0$. If $U_{D_2,1}$ from a sphenoid or a regular tetrahedron, when $\epsilon = 0$, $U_{D_2,1}$ forms a regular tetrahedron or a sphenoid in the base polyhedron (a regular icosahedron). There are two types of possibilities for the edges of these regular tetrahedron or a sphenoid in the base polyhedron: the edges of the regular icosahedron or the edges in the interior of the regular icosahedron connecting two vertices. For any edge of the regular icosahedron, we cannot find any vertex on the 2-fold axis of it. For the edges in the interior of the regular icosahedron, there are two possibilities as shown in Figure 21, but we cannot find any vertex on the 2-fold axis of it. When $\epsilon > 0$, the arrangement of edges of $U_{D_2,1}$ slightly moves from the regular tetrahedron or the sphenoid, but we cannot find two points forming $U_{D_2,2}$ on the 2-fold axis of $U_{D_2,1}$.

In the same way, if $U_{D_2,1}$ forms a rectangle or a square, when $\epsilon = 0$, $U_{D_2,1}$ forms a line formed by two vertices of the base polyhedron or a rectangle formed by four vertices of the base polyhedron. The possible edges are same as the previous case and in the same way, we cannot find any $U_{D_2,2}$. Hence $\gamma(P') \neq D_2, C_2$.

Assume $\gamma(P') = D_5$, then P' contains at least one regular pentagon. Figure 22 shows all possible regular pentagons in D and any regular pentagon in D is centered at a 5-fold axis of $\gamma(D) = I$.

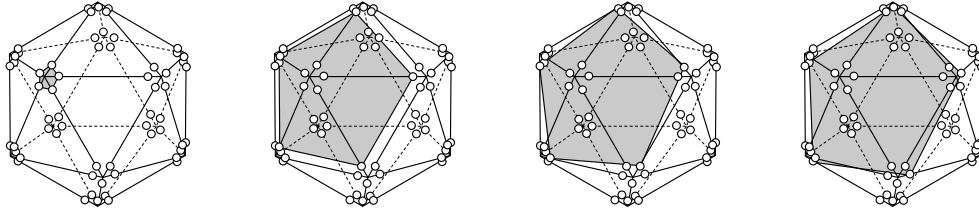


Fig. 22. Regular pentagons in an ϵ -truncated icosahedron.

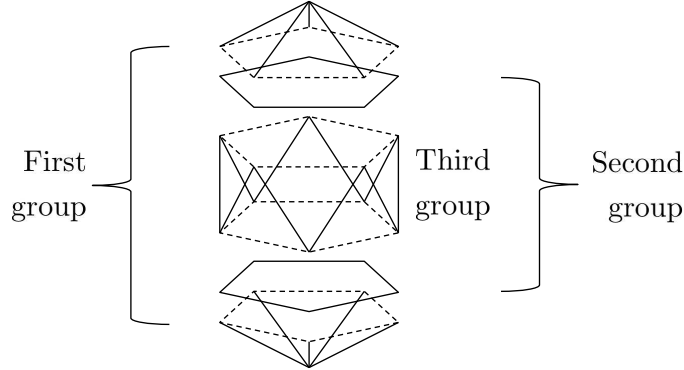


Fig. 23. Decomposition of the edges of an ϵ -truncated icosahedron around a 5-fold axis by using the base polyhedron. The bold edges show the member edges of each group.

Because there is no point of D on the 5-fold axis of any regular pentagon, the D_5 -decomposition of P' does not contain $U_{D_5,5}$.

Assume that the D_5 -decomposition of P' consists of three $U_{D_5,1}$'s (cardinality 10). Thus the three $U_{D_5,1}$'s share a 5-rotation axis of $\gamma(D)$. We divide the long edges of the ϵ -truncated icosahedron into three groups base on a decomposition of the base polyhedron into two regular pentagonal pyramids and one pentagonal anti-prism. The first group consists of the side edges of the two pyramids, the second group consists of the perimeter of the bases of the pyramids (also the anti-prism), and the third group consists of the side edges of the anti-prism as shown in Figure 23.

Remember that the two endpoints of each long edge of the ϵ -truncated icosahedron are the destinations of one robot and P' contains just one of them. From the endpoints of the first group, we can construct at most one pentagonal anti-prism (i.e., $U_{D_5,1}$) and from the second group, we can construct at most one pentagonal anti-prism. Then we check the endpoints of the third group and we can form two pentagonal anti-prisms each of which contains both endpoints of long edges of D because the anti-prisms should share an arrangement of D_5 with the pentagonal anti-prisms formed by the first and the second groups. Thus P' cannot contain three $U_{D_5,1}$'s.

Assume that the D_5 -decomposition of P' contains $U_{D_5,2}$ (cardinality 5). Because $|P'| = 30$, the number of $U_{D_5,2}$'s is even and from Figure 22, at most two regular pentagons from D are on the same plane. Thus we have two $U_{D_5,2}$'s and two $U_{D_5,1}$'s. The bases of $U_{D_5,1}$'s are selected from the pentagons in Figure 22 and opposite against the plane containing the two $U_{D_5,2}$'s, but we cannot find any two $U_{D_5,2}$'s on such a plane. Thus we do not have this case. Hence $\gamma(P') \neq D_5$.

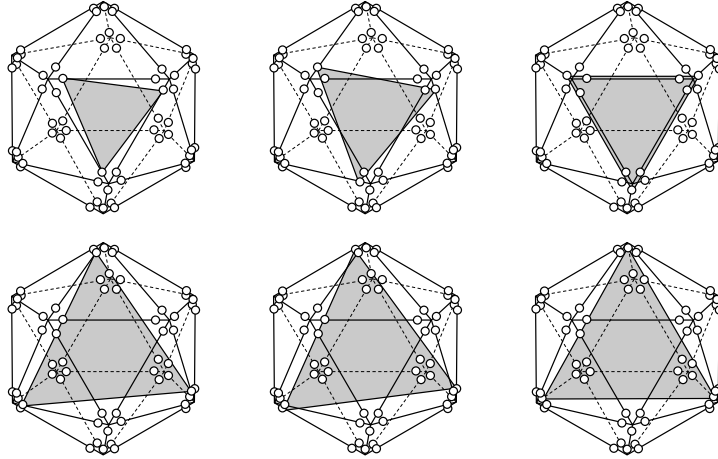


Fig. 24. Regular triangles in an ϵ -truncated icosahedron.

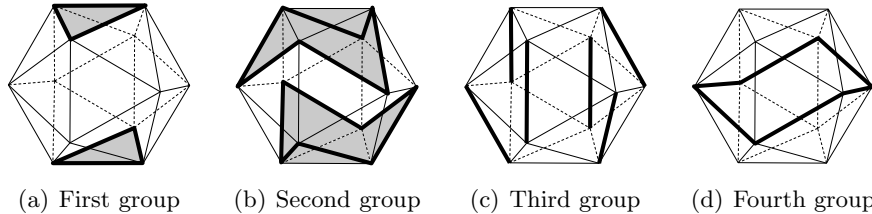


Fig. 25. Decomposition of the edges of an ϵ -truncated icosahedron around a 3-fold axis by using the base polygon. The bold edges show the member edges of each group.

Assume $\gamma(P') = D_3$, then P' contains at least one regular triangle. On the other hand, it does not contain $U_{D_3,3}$ (cardinality 2). Figure 24 shows all regular triangles in D and any regular triangle in D is centered at a 3-rotation axis of $\gamma(D) = I$. Hence there is no point on the 3-fold axis of any regular pentagon in D and the D_3 -decomposition of P' does not contain $U_{D_3,3}$.

Assume that the D_3 -decomposition of P' consists of five $U_{D_3,1}$'s. Hence the five $U_{D_3,1}$'s share a 3-rotation axis of $\gamma(D)$. We divide the long edges of the ϵ -truncated icosahedron based on a decomposition of the edges of a regular icosahedron into four groups as shown in Figure 25.

Remember that the two endpoints of each long edge of the ϵ -truncated icosahedron are the destinations of one robot and P' contains just one of them. From the endpoints of the first group, we can construct at most one triangular anti-prism (i.e., $U_{D_3,1}$). In the same way, we can construct at most two triangular anti-prisms and at most one triangular anti-prism from the second and the third group. Then we check the endpoints of the fourth group and we can form two triangular anti-prisms each of which contains both endpoints of long edges of D because they should share the arrangement of D_3 with $U_{D_3,1}$'s formed by the other groups. Thus P' does not contain five $U_{D_3,1}$'s.

Assume that the D_3 -decomposition of P' contains $U_{D_3,2}$, then because $|P'| = 30$, the number of $U_{D_3,2}$ in the D_3 -decomposition of P' is even and they are on the same plane. From Figure 24, at most two triangles from D are on the same plane. Thus we have two $U_{D_3,2}$'s and four $U_{D_3,1}$'s. The bases of $U_{D_3,1}$'s are selected from the regular triangles in Figure 24 and opposite against the

plane containing the two $U_{D_{3,2}}$'s, but we cannot find any two $U_{D_{3,2}}$'s on such a plane. Thus we do not have this case. Hence $\gamma(P') \neq D_3$.

We check the 3D rotation groups. First, assume $\gamma(P') = T$, then the T -decomposition of P' contains at least one $U_{T,2}$ (cardinality 6) because $|P'| = 30$ is not divided by 4. Because the vertices of an ϵ -truncated icosahedron is around the vertices of a regular icosahedron, we cannot find any regular octahedron in D . Hence, $\gamma(P) \neq T$.

Second, assume $\gamma(P') = O$, then the O -decomposition of P' contains at least one $U_{O,4}$ (cardinality 6) since $|P'| = 30$ is not divided by 4. In the same way as the previous case, we cannot find any regular octahedron in D . Hence $\gamma(P) \neq O$.

Finally, assume $\gamma(P') = I$, then the I -decomposition of P' forms $U_{I,2}$ (cardinality 30) since $|P'| = 30$. Because the vertices of an ϵ -truncated icosahedron is around the vertices of a regular icosahedron, we cannot find any icosidodecahedron in D . Hence $\gamma(P) \neq I$.

Consequently, $\gamma(P') \preceq C_3$ or C_5 . □

4.2 Composition of transitive sets of points

In this section, we show algorithm ψ_{SYM} that translates an initial configuration P to another configuration P' that satisfies $\gamma(P') \in \varrho(P)$. When P is transitive regarding a 3D rotation group, ψ_{SYM} makes the robots execute the “go-to-center” algorithm (Algorithm 4.1) and its correctness is already shown in Section 4.1. In this section, we consider other initial configurations where $\gamma(P) \notin \varrho(P)$.

For example, consider the case where P consists of a cube and a regular octahedron with $\gamma(P) = O$ (Figure 26(a)). In this case, unoccupied rotation axes are the six 2-fold axes, and $\varrho(P) = \{C_2\}$, because there are no three 2-fold axes perpendicular to each other. As we have already shown, each of these regular polyhedra can show its symmetricity by executing Algorithm 4.1 and the robots on the 3-fold axes and 4-fold axes eliminate these rotation axes. However there are executions that do not keep the the smallest enclosing ball of the robots (Figure 26(b)) and we cannot directly discuss the composite symmetricity. Rather, algorithm ψ_{SYM} makes each element of the $\gamma(P)$ -decomposition show its symmetricity one by one with keeping the smallest enclosing ball unchanged. For example, starting from an initial configuration shown in Figure 26(a), the proposed algorithm first makes the robots forming a regular octahedron execute the go-to-center algorithm with the robots forming a cube keeping the smallest enclosing circle. Let P' be the configuration after the regular octahedron is broken. Because the robots formed the regular octahedron approaches to the center, the robots forming the cube do not move during the transition from P to P' and they also keep the rotation axes of P , i.e., any rotation applicable to P' should also applicable to the cube. Hence, we can check $\gamma(P')$ by checking the rotation axes of O . For example, because a robot on a 4-fold axes in P (i.e., a robot forming a regular octahedron) left the rotation axes and there are no three corresponding robots to keep the rotation axes, $\gamma(P')$ does not have any 4-rotation axes. Hence, $\gamma(P') \preceq D_3$. When $\gamma(P') = D_3$, P' is a configuration where the principal rotation axis is occupied by two robots forming the cube. The robots can translate P' to another configuration P'' with $\gamma(P'') \preceq C_2$ by the two robots leaving the principal axis. Other possibility is $\gamma(P') = C_3$, the robots can recognize a single robot on the single rotation axis and the robots can translate P' to P'' where $\gamma(P'') = C_1$ by this robot leaving the axis. In this way, the robots can translate P to another configuration P'' that satisfies $\gamma(P'') \preceq C_2 \in \varrho(P)$.

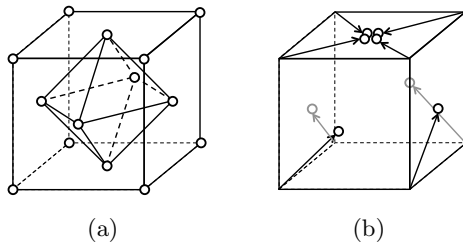


Fig. 26. Symmetry breaking from a composite initial configuration.

Algorithm ψ_{SYM} The proposed algorithm ψ_{SYM} is shown in Algorithm 4.2. Algorithm ψ_{SYM} makes the robots on each type (i.e., fold) of the rotation axes leave the positions by repeating the following procedure: ψ_{SYM} first selects an element of the $\gamma(P)$ -decomposition of the current configuration P that is on the rotation axes $\gamma(P)$ and make the element shrink toward $b(P)$ so that the other robots keep the smallest enclosing ball (Procedure `shrink` in Algorithm 4.3). This movement does not change the rotation group of the positions of robots. Let P' be a resulting configuration. Then, ψ_{SYM} makes the innermost robots leave the rotation axes of $\gamma(P')$. Depending on $\gamma(P')$, there are three procedures; go-to-sphere (when $\gamma(P')$ is cyclic or $\gamma(P')$ is dihedral and its principal axis is occupied), go-to-corner (when $\gamma(P')$ is dihedral and its secondary axes are occupied,) go-to-center (Algorithm 4.1, when $\gamma(P')$ is a 3D rotation group). These three procedures send the robots on $I(P')$ to some point in the interior of $I(P')$ and not on any rotation axes of $\gamma(P')$. By repeating these two phases, ψ_{SYM} removes occupied rotation axes.

Any terminal configuration P of Algorithm 4.2 satisfies one of the following two properties:

- (i) If $\gamma(P) \neq C_1$, then P is a regular n -gon or no robot is on the rotation axes of $\gamma(P)$.
- (ii) $\gamma(P) = C_1$.

When an arbitrary configuration P satisfies one of the above two conditions, ψ_{SYM} outputs \emptyset at all robots. For any terminal configuration P , the $\gamma(P)$ -decomposition of P consists of elements of size $|\gamma(P)|$, which is shown to be useful in the pattern formation algorithm in Section 6. Here, C_1 -decomposition of P divides P into n subsets.

In ψ_{SYM} , we use the following notations. Let P and $\{P_1, P_2, \dots, P_m\}$ be an initial configuration and its $\gamma(P)$ -decomposition.

- P_{ip} : The element on the (principal) axis when $\gamma(P)$ is cyclic or dihedral. If there are multiple such elements, ψ_{SYM} selects the element with the minimum index.
- P_{is} : The element on the secondary axis when $\gamma(P)$ is dihedral. If there are multiple such elements, ψ_{SYM} selects the element with the minimum index.
- P_{imax} : The element on some occupied rotation axes with the maximum fold when $\gamma(P) \in \{T, O, I\}$. If there are multiple such elements, ψ_{SYM} selects the element with the minimum index.

For example, if P consists of a regular octahedron and a cube (Figure 26(a)), all the 3-fold axes and 4-fold axes are occupied, and P_{imax} is the element forming the regular octahedron. The robots can agree on P_{ip} , P_{is} , and P_{imax} if any irrespective of local coordinate systems.

When $\gamma(P)$ is dihedral, ψ_{SYM} uses the *reference prism* that inscribed in a ball $Ball(b(P), rad(I(P))/2)$. Consider a cylinder with radius is $rad(I(P)/4)$ that is parallel to the principal axes and inscribed in

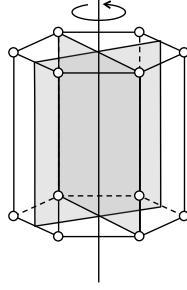


Fig. 27. Reference prism for D_6 . There are 6 planes formed by the principal axes and a 2-fold axes, and the reference prism consists of regular 12-gon faces.

$I(P)$. The corners of the reference prism are the intersection of this cylinder and the plane formed by the principal axes and a secondary axes (Figure 27). Hence, when $\gamma(P) = D_k$, the bases of the reference prism are regular $2k$ -gons.

Correctness of ψ_{SYM} We show the correctness of Algorithm 4.2. Let $P(0), P(1), P(2), \dots$ be an execution of Algorithm 4.2 from an initial configuration $P(0)$. If $P(0)$ is transitive, Algorithm 4.2 executes Algorithm 4.1 and its correctness is already shown in Section 4.1. In the following, we assume that $P(0)$ is not transitive and $\gamma(P(0))$ -decomposition of $P(0)$ consists of at least two elements. We first show that ψ_{SYM} does not allow the robots to form one transitive set of points and for any $t \geq 0$, $\gamma(P(t))$ -decomposition of $P(t)$ consists of at least two elements (Lemma 8).

For each transition from $P(t)$ to $P(t+1)$, if some robots move, they execute one of the five procedures **Expand**, **Shrink**, **go-to-sphere**, **go-to-corner** (shown in Algorithm 4.3) and **go-to-center** (Algorithm 4.1). The moving robots execute the same procedure, because they can agree on $\gamma(P(t))$ and the $\gamma(P(t))$ -decomposition of $P(t)$ that determines the procedure they execute.

We will show that the rotation axes occupied by robots in $P(0)$ are gradually eliminated without adding any new rotation axis. Let $\gamma^+(P(t))$ ($\gamma^-(P(t))$, respectively) be the arrangement of occupied rotation axes (unoccupied rotation axes) of $\gamma(P(t))$. We also consider each of them as a set of rotation axes. In the following, we focus not on the fold of a rotation axes, but on the existence of the rotation axes. Even when the fold of a rotation axis becomes smaller, during a transition from $P(t)$ to $P(t+1)$, we say the rotation axis remains in $\gamma(P(t+1))$.

We will show the following two properties.

1. When robots execute **go-to-sphere**, **go-to-corner**, or **go-to-center**, $\gamma^+(P(t+1))$ is a proper subset of $\gamma^+(P(t))$.
2. $\gamma^-(P(t+1))$ is a subset of $\gamma^-(P(t))$.

Starting from an initial configuration $P(0)$, the first property guarantees that all occupied rotation axes are gradually eliminated because ψ_{SYM} executes these three procedures as long as there is an occupied rotation axis. The second property guarantees that the movement of robots does not add any new rotation axis. Hence the robot system eventually reaches a configuration $P(t^*)$ that have no occupied rotation axes and $\gamma(P(t^*)) \preceq \gamma^-(P(0))$. This property of $\gamma(P(t^*))$ satisfies the definition of the symmetricity and ψ_{SYM} succeeds in making robots show their symmetricity.

Lemma 8. *Let $P(0), P(1), P(2), \dots$ be an execution of Algorithm 4.2 by oblivious FSYNC robots from an initial configuration $P(0)$. If $P(0)$ is not transitive, then $P(t)$ is not transitive for all $t \geq 0$.*

Algorithm 4.2 ψ_{SYM} for robot $r_i \in R$

Notation

P : The positions of robots observed in Z_i .
 $\{P_1, P_2, \dots, P_m\}$: $\gamma(P)$ -decomposition of P .
 p_i : current position of r_i .

Algorithm

```
If  $p_i = b(P)$  then
  Execute go-to-sphere
Else
  If  $\gamma(P) \neq C_k$  and  $P \cap B(P) \neq P_m$  then
    If  $p_i \in P_m$  then
      Execute Expand
      // To guarantee that there are at least two robots on the smallest enclosing ball of the robots.
    Endif
  Else
    Switch ( $\gamma(P)$ ) do
      Case  $C_k$  ( $k \geq 1$ ):
        If  $k \neq 1$  and  $P_{ip}$  is determined and  $p_i \in P_{ip}$  then
          If  $P_{ip} \neq P_1$  then
            Execute Shrink( $P \setminus P_{ip}$ ).
          Else
            Execute go-to-sphere
          Endif
        Endif
      Case  $D_\ell$  ( $\ell \geq 2$ ):
        If  $P_{ip}$  is determined and  $p_i \in P_{ip}$  then
          If  $P_{ip} \neq P_1$  then
            Execute Shrink( $P$ ).
          Else
            Execute go-to-corner
          Endif
        Else
          If  $P_{is}$  is determined,  $P \neq P_{is}$  and  $p_i \in P_{is}$  then
            If  $P_{is} \neq P_1$  then
              Execute Shrink( $P$ ).
            Else
              Execute go-to-corner
            Endif
          Endif
        Default //  $\gamma(P) \in \{T, O, I\}$ :
          If  $P_{imax}$  is determined and  $p_i \in P_{imax}$  then
            If  $P_{imax} \neq P_1$  then
              Execute Shrink( $P$ ).
            Else
              Execute go-to-center( $P_{imax}$ ) // Algorithm 4.1.
            Endif
          Endif
        Enddo
      Endif
    Enddo
  Endif
Endif
```

Algorithm 4.3 Procedure for Algorithm 4.2

Expand

Let d_i be the intersection of $Ball(b(P), 2rad(I(P)))$ and the half line from $b(P)$ that passes p_i .
Go to d_i .

Shrink(Q)

Let d_i be the intersection of $Ball(b(Q), I(Q)/2)$ and the line $\overline{p_i b(Q)}$.
Go to d_i .

go-to-sphere

Select arbitrary point on $Ball(b(P), rad(I(P)/2)$ with avoiding the intersections with rotation axes of $\gamma(P)$ and the equator (if $\gamma(P)$ is a 2D rotation group).
Move to the point.

go-to-corner

Select a nearest vertex of the reference prism.
Go to the selected vertex.

Proof. Let $\{P_1(t), P_2(t), \dots, P_{m(t)}(t)\}$ be the $\gamma(P(t))$ -decomposition of $P(t)$. Because ψ_{SYM} outputs nothing at any robot when $\gamma(P(t)) = C_1$, we assume $\gamma(P(t)) \neq C_1$. Hence, each $Ball(P_i(t))$ is a ball centered at $b(P(t))$. We will show that ψ_{SYM} does not move any $P_i(t)$ to $Ball(P_j(t))$ for any $i \neq j$.

When $t = 0$, from the assumption, $P(0)$ is not transitive and the $\gamma(P(0))$ -decomposition of $P(0)$ consists of at least two elements. Assume ψ_{SYM} selects $P_i(0)$ to move the robots forming it. Then these robots synchronously execute one of the five procedures, **Expand**, **Shrink**, **go-to-sphere**, **go-to-corner**, and **go-to-center**. When these robots execute **Expand**, they move to the exterior of $B(P(0))$. In the same way, when they execute **Shrink**, they move to the interior of $I(P(0))$. When they execute **go-to-sphere**, **go-to-corner**, or **go-to-center**, they are on $I(P(0))$ and their destinations are also in the interior of $I(P(0))$. Hence during the transition from $P(0)$ to $P(1)$, ψ_{SYM} does not move any $P_i(0)$ to $Ball(P_j(0))$ for any $i \neq j$.

In the same way, for any transition from $P(t)$ to $P(t+1)$, ψ_{SYM} does not move any $P_i(t)$ to $Ball(P_j(t))$ for any $i \neq j$, because the destinations of the five procedures are selected based on $I(P(t))$ and $B(P(t))$. Hence we obtain the lemma. \square

Lemma 9. *Let $P(0), P(1), P(2), \dots$ be an execution of Algorithm 4.2 by oblivious FSYNC robots from a non transitive initial configuration $P(0)$. If some robots execute **Shrink** or **Expand** during the transition from $P(t)$ to $P(t+1)$, then we have $\gamma^+(P(t+1)) = \gamma^+(P(t))$ and $\gamma^-(P(t+1)) = \gamma^-(P(t))$.*

Proof. As already mentioned, the robots that execute **Shrink** or **Expand** during the transition from $P(t)$ to $P(t+1)$ form an element of the $\gamma(P(t))$ -decomposition of $P(t)$, and they agree on which procedure they execute. Let R' and P' be the set of robots that execute one of these two procedures during the transition from $P(t)$ to $P(t+1)$, and their positions in $P(t)$.

If **Shrink** is executed, because the movement of robots of R' are radial against $b(P(t))$, it does not add any new rotation axis to $\gamma(P(t))$. On the other hand, there is at least another element of the $\gamma(P(t))$ -decomposition of $P(t)$ in $P(t) \setminus P'$ and they keep the rotation axes of $P(t)$. When $\gamma(P(t))$ is cyclic, there is another element that forms $U_{\gamma(P(t)),1}$ (otherwise $\gamma(P(t))$ is not cyclic), and keeps the rotation axes of $\gamma(P(t))$. When $\gamma(P(t))$ is dihedral, there is another element that forms $U_{\gamma(P(t)),1}$ or $U_{\gamma(P(t)),2}$ (otherwise $\gamma(P(t))$ is not dihedral), and keeps the rotation axes of

$\gamma(P(t))$. When $\gamma(P(t)) \in \{T, O, I\}$, there is another element that forms $U_{\gamma(P(t)), \mu}$ for $\mu < |\gamma(P(t))|$ and keeps the rotation axes of $\gamma(P(t))$. Hence this movement of R' does not change the occupied and unoccupied rotation axis.

If **Expand** is executed, $\gamma(P(t))$ is a dihedral group or a 3D rotation group. In the same way, the movement is radially against $b(P(t))$, and it does not change the rotation group and occupied and unoccupied rotation axes. \square

Lemma 10. *Let $P(0), P(1), P(2), \dots$ be an execution of Algorithm 4.2 by oblivious FSYNC robots from a non transitive initial configuration $P(0)$. If some robots execute **go-to-center**, **go-to-corner**, or **go-to-sphere** during the transition from $P(t)$ to $P(t+1)$, then we have $\gamma^+(P(t+1)) \subset \gamma^+(P(t))$ and $\gamma^-(P(t+1)) \subseteq \gamma^-(P(t))$.*

Proof. As already mentioned, robots that move during the transition from $P(t)$ to $P(t+1)$ form the first element of the $\gamma(P(t))$ -decomposition of $P(t)$, and execute the same procedure selected from the three procedures **go-to-center**, **go-to-corner**, or **go-to-sphere**. Let R' be the set of these moving robots.

From Lemma 8, $P(t)$ is not transitive and there exists at least one another element of the $\gamma(P(t))$ -decomposition of $P(t)$ that does not move during the transition. and keep $B(P(t))$. Clearly, $\gamma(B(P(t)) \cap P(t)) = \gamma(P(t))$. No robot moves to the sphere of $B(P(t))$ during the transition because the robots of R' moves to the interior of $I(P(t))$. Hence if we can apply some rotation to $P(t+1)$, then we can also apply it to $P(t+1) \cap B(P(t+1))$. In other words, $\gamma(P(t+1)) \preceq \gamma(P(t))$.

We first show $\gamma^+(P(t+1)) \subset \gamma^+(P(t))$. Observe that the three procedures **go-to-center**, **go-to-corner**, and **go-to-sphere** assigns candidate destinations to each robot in $P(t)$ so that the set of candidate destinations of robots in $P(t)$ are disjoint. Let a be the rotation axes that is occupied by a robot r that executes one of these three procedures. To keep this axes a in $P(t+1)$, at least one point that is symmetric for the destination of r regarding axes a should be occupied by another robot in $P(t+1)$. Such a point is a candidate destination of r and no robot will occupy this point. Hence, $\gamma(P(t+1))$ does not have this rotation axes. Hence, $\gamma^+(P(t+1)) \subset \gamma^+(P(t))$.

Additionally, the three procedures **go-to-corner**, **go-to-center**, **go-to-sphere** do not allow the robots to move a point on the rotation axis of $\gamma(P(t))$. Hence, the unoccupied rotation axes of $\gamma(P(t))$ remains unoccupied in $P(t)$. Thus, we have $\gamma^-(P(t+1)) \subseteq \gamma^-(P(t))$.

Consequently, $P(t+1)$ satisfies the two properties. \square

Theorem 3. *Let P be an arbitrary initial configuration of oblivious FSYNC robots. Algorithm 4.2 translates P into another configuration P' that satisfies the terminal condition of ψ_{SYM} and $\gamma(P) \in \rho(P)$ in at most 7 steps.*

Proof. Let $P(0)(= P), P(1), P(2), \dots$ be the execution of Algorithm 4.2 from P . In the worst case, one of the three procedures **go-to-center**, **go-to-corner**, **go-to-sphere** is executed in every two steps, with the exception that for the first and the second cycle the robots execute **Expand** and **Shrink**. From Lemma 10, every time the three procedures are executed, at least one type of occupied rotation axes are eliminated without increasing the occupied rotation axes. Hence, the system eventually reaches a configuration $P(t^*)$ where $\gamma^+(P(t^*))$ is empty. Additionally, Lemma 10 guarantees

$$\gamma^-(P(t^*)) = \gamma(P(t^*)) \subseteq \gamma(P(t^* - 1)) \subseteq \dots \subseteq \gamma(P(0)).$$

Hence, $P(t^*)$ satisfies the claim.

In the worst case, $t^* = 7$ because in each iteration, just one type of rotation axes is eliminated. \square

5 Necessity of Theorem 1

In this section, we prove the necessity of Theorem 1.

Theorem 4. *Regardless of obliviousness, FSYNC robots can form a target pattern F from an initial configuration P only if $\varrho(P) \subseteq \varrho(F)$.*

To prove Theorem 4, we show the following lemma on the relationship between $\sigma(P)$ and $\varrho(P)$ of a configuration P without multiplicity.

Lemma 11. *For a configuration P without multiplicity, $\sigma(P) \in \varrho(P)$.*

Proof. The proof is by Property 5. □

Lemma 12. *Oblivious FSYNC robots can form a target pattern F from an initial configuration P only if $\varrho(P) \subseteq \varrho(F)$.*

Proof. Let P and F be a given initial configuration and a target pattern without multiplicity that does not satisfy $\varrho(P) \subseteq \varrho(F)$. Hence there exists $G \in \varrho(P)$ such that $G \notin \varrho(F)$.

Assume that there exists an algorithm ψ that forms F from P , for contradiction. Consider an initial arrangement of local coordinate systems that satisfies $\sigma(P) = G$. Such arrangement exists from the definition. From the assumption, there exists at least one execution $P(0)(= P), P(1), P(2), \dots$ that satisfies $P(t) \simeq F$ for some $t > 0$. From Lemma 2, we have $\sigma(P(t)) \succeq \sigma(P(0)) = G$.

From the definition of the symmetricity, we have the following: if $G' \in \varrho(F)$, any subgroup of G' is in $\varrho(F)$. In other words, if there exists a subgroup of G' that is not in $\varrho(F)$, then $G' \notin \varrho(F)$. Because $\sigma(P(0)) = G$ is not in $\varrho(F)$, its supergroup $\sigma(P(t))$ is not in $\varrho(F)$.

This contradicts Lemma 11 that guarantees $\sigma(P(t)) \in \varrho(P(t))$. □

In the same way, we have the non-oblivious robot version directly from Lemma 3. Consequently, we have Theorem 4.

6 Sufficiency of Theorem 1

We have shown that the necessity is derived from the symmetricity of an initial configuration. We will show that the condition of Theorem 4 is also a sufficient condition for FSYNC robots to form a given target pattern.

Theorem 5. *Regardless of obliviousness, FSYNC robots can form a target pattern F from an initial configuration P if $\varrho(P) \subseteq \varrho(F)$.*

We present a pattern formation algorithm ψ_{PF} that makes oblivious FSYNC robots form a target pattern F from a given initial configuration P if P and F satisfy the condition of Theorem 5. Non-oblivious robots can also execute ψ_{PF} correctly by ignoring local memory contents.

As we have already seen in Section 4, algorithm ψ_{SYM} translates an initial configuration P to another configuration P' that satisfies (i) $\gamma(P') \in \varrho(P)$, (ii) If $\gamma(P') \neq C_1$, then P' is a regular n -gon or no robot is on the rotation axes of $\gamma(P')$. Let $\{P'_1, P'_2, \dots, P'_m\}$ be the $\gamma(P')$ -decomposition of P' . From the first property, we have $\gamma(P') \in \varrho(F)$. From the second property, the size of each element $|P'_i|$ ($1 \leq i \leq m$) is $|\gamma(P')|$. The second property implies $\sigma(P') = \gamma(P')$ in the worst case

and the robots forming each element of the $\gamma(P')$ -decomposition of P' may forever move symmetric positions regarding $\gamma(P')$.

The proposed pattern formation algorithm ψ_{PF} first makes the robots agree on an embedding of F in P' so that $\gamma(P')$ overlaps unoccupied rotation axes of $\gamma(F)$. Because $\gamma(P') \in \varrho(F)$, such embedding exists and it guarantees that $\gamma(P')$ -decomposition of F consists of elements of size $|\gamma(P')|$. Thus we can overcome the symmetric movement of each element of the $\gamma(P')$ -decomposition of P' by assigning it to an element of the $\gamma(P')$ -decomposition of F . We denote the embedded target pattern by \tilde{F} . Then ψ_{PF} makes them compute a perfect matching between P' and \tilde{F} , denoted by $M(P, \tilde{F})$ to assign final destination to each robot.

We will show how the robots agree on \tilde{F} in Section 6.1 and on the perfect matching between P' and \tilde{F} in Section 6.2.

6.1 Embedding the target pattern

Let P be a current configuration that is a terminal configuration of ψ_{SYM} and no rotation axis of P is occupied unless P is on one plane. From the condition of Theorem 5, $\gamma(P) \in \varrho(F)$.

To form the target pattern F , the robots first fix an image of the target pattern F . We denote this image by \tilde{F} . The robots fix \tilde{F} so that $B(\tilde{F}) = B(P)$ and unoccupied rotation axes of $\gamma(\tilde{F})$ overlaps the rotation axes of $\gamma(P)$. Algorithm ψ_{PF} first fixes the arrangement of $\gamma(F)$ in P instead of \tilde{F} . The robots construct an agreement on the arrangement of rotation axes of $\gamma(F)$ that $\gamma(P)$ does not have. In the following, we refer to an arrangement of a rotation group G by using $U_{G,\mu}$ for some $\mu > 1$ because it helps our understanding with illustration. Depending on $\gamma(P)$, we have the following two cases.

When $\gamma(P)$ is a 3D rotation group. We have only two cases to consider because $O \not\leq I$, i.e, the first case is when $\gamma(P) = T$ and $\gamma(F) = O$ and the second case is when $\gamma(P) = O$ and $\gamma(F) = I$.

First, when $\gamma(P) = T$ and $\gamma(F) = O$, the 3-fold axes and 4-fold axes of $\gamma(F)$ are not occupied, otherwise $T \notin \varrho(F)$. The robots fix the arrangement of O in T as shown in Figure 28(a): ψ_{PF} replace the 2-fold axes of T with 4-fold axes of O . The set of 3-fold axes of T and new 4-fold axes generate the remaining 2-fold axes of O .¹¹ Thus the rotation axes of $\gamma(P)$ corresponds to the 3-fold axes and the 4-fold axes of $\gamma(F)$ and $\gamma(P)$ overlaps unoccupied rotation axes of $\gamma(F)$.

Second, when $\gamma(P) = T$ and $\gamma(F) = I$, the 3-fold axes and 2-fold axes of $\gamma(F)$ are not occupied, otherwise $T \notin \varrho(F)$. The robots first fix the arrangement of O in T , then further add some rotation axes to fix the arrangement of I . We use the orientation of the 3-fold axes of T in this procedure. The robots extend T to O in the same way as the previous case and consider a unit cube (in their local coordinate systems). Then they put two types of 3-blade fan components to each of the vertices of the cube (Figure 28(b)). The two types of fans are mirror image of each other and we call one of them “black” and the other “white”. The robots put a black component on the vertex of the cube on the positive direction of the 3-fold axis of T (the vertices of the regular tetrahedron in Figure 28(b)) and a white component on the vertex of the cube on the negative direction of the 3-fold axis of T . We need such procedure because there are two types of embeddings of a cube to a regular dodecahedron (thus, the arrangement of I) (Figure 28(c) and Figure 28(d)), and robots have to agree on one of the two arrangements of I . The rotation axes of $\gamma(P)$ corresponds to the 3-fold axes and the 2-fold axes of $\gamma(F)$ and $\gamma(P)$ overlaps unoccupied rotation axes of $\gamma(F)$.

In the above two cases, once $\gamma(F)$ is fixed, \tilde{F} is also fixed with the condition that $B(\tilde{F}) = B(P')$.

¹¹ Because the rotation around the 4-fold axes and the 3-fold axes are the generator of O .

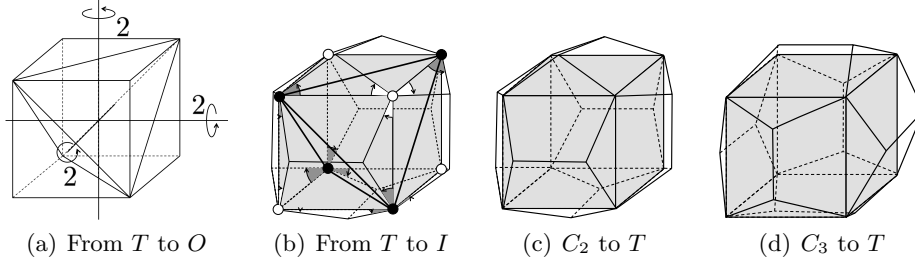


Fig. 28. Fixing $\gamma(F)$ in $\gamma(P')$. Instead of drawing rotation axes, we show a typical regular polyhedron for $\gamma(F)$ that shows the arrangement of rotation axes of $\gamma(F)$.

When $\gamma(P)$ is a 2D rotation group. In this case, we cannot always fix $\gamma(F)$ by using only the rotation axes of $\gamma(P)$. Consider the case where $\gamma(P) = C_k$ and $\gamma(F) = D_k$ for some positive integer k . In this case, the robots cannot agree on the arrangement of secondary axes of D_k by using only the single rotation axis of C_k . In such cases, we use the positions of point of P to fix the rotation axes of $\gamma(F)$. A *reference polygon* of P for a specified k -fold axis of $\gamma(P)$ is a regular k -gon on a plane that is perpendicular to $\gamma(P)$ and contains $b(P)$.¹² We consider the specified axis as the earth's axis of $B(P)$ and consider the *equator plane* for the axis. Thus the reference polygon is on the equator plane.

We also consider a reference polygon of F in the same way. The role of the reference polygon is twofold; one is for P to show reference points when fixing an arrangement of additional rotation axes and the other is for F to recover all the arrangement of rotation axes when given the specified rotation axes and its reference polygon.

Specifically, the robots agree on the reference polygon as follows:

Case A. $\gamma(P) = C_k$. In this case, there is only the single rotation axis. Let $\{P_1, P_2, \dots, P_m\}$ be the $\gamma(P)$ -decomposition of P . When $k \geq 2$, there exists at least one element in the $\gamma(P)$ -decomposition of P that form a regular k -gon perpendicular to the single rotation axis. Let P_i be the element that has the minimum index among such elements. Then the reference polygon is the projection of the regular k -gon formed by P_i onto the equator plane.

When $\gamma(P) = C_1$, each element of the $\gamma(P)$ -decomposition is a 1-set. Let $P_1 = \{p_1\}$. Because $\gamma(P) = C_1$, there is at least one element that is not on the line containing $b(P)$ and p_1 . Let $P_i = \{p_i\}$ be the element with the minimum index among such elements. Then the reference polygon is the projection of p_i onto the equator plane.

Case B. $\gamma(P) = D_\ell$. In this case, there are two choices for the rotation axis for the reference polygon. However, we do not have to consider the secondary axis of $\gamma(P)$ because $\gamma(P) \preceq \gamma(F)$, $\gamma(F)$ has a rotation axis whose fold is a multiple of ℓ , and ψ_{PF} makes the principal axis of D_ℓ overlap such rotation axis of $\gamma(F)$.

Let $\{P_1, P_2, \dots, P_m\}$ be the $\gamma(P)$ -decomposition of P . When the $\gamma(P)$ -decomposition of P contains $U_{D_\ell, 2}$, the reference polygon is defined by the element with the minimum index among such elements because such regular ℓ -gon is on the equator plane. Otherwise, the $\gamma(P)$ -decomposition of P contains at least one $U_{D_\ell, 1}$ and let P_i be the element with the minimum index among such elements. When P_i forms a regular prism, the reference polygon is defined by the projection of the bases onto the equator plane. When P_i is not a regular prism, the robots consider twisting the

¹² When the principal axis of a dihedral group D_ℓ is specified, the reference polygon also determines the orientation of secondary axis if ℓ is odd.

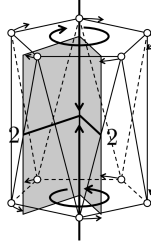


Fig. 29. Twisting $U_{D_5,1}$ to form a pentagonal prism.

bases so that the vertices overlap the nearest plane formed by a 2-fold axis and the principal axis of $\gamma(P)$. The twist follows the right screw rule with considering the direction from a base to $b(P)$ as the positive direction (Figure 29). This twisting enables the robots agree on a regular prism and the reference polygon is defined in the same way as the above case.

Case C. $\gamma(F)$ is cyclic or dihedral. In this case, when the single rotation axis or the principal axis is specified, the reference polygon is defined in the same way as Case A and B.

When $\gamma(F)$ is dihedral and a secondary axis is specified, the reference polygon is defined by the intersection of the principal axis and the equator.

Case D. $\gamma(F) \in \{T, O, I\}$. There are three rotation axes to define a reference polygon because $\gamma(F)$ consists of three types of rotation axes. Figure 30 shows reference polygons for each type of the rotation axis. Readers can easily find that the reference polygons are defined in the same way as Case B, specifically, when the specified rotation axis is oriented, the reference polygon is defined in the same way as when $\gamma(F)$ is cyclic (Figure 30(b)) and when the specified rotation axis is not oriented, it is defined in the same way as when $\gamma(F)$ is dihedral. Find that with the specified rotation axis and its reference polygon, we can uniquely fix the arrangement of all other rotation axes of $\gamma(F)$.

Now we describe how the robots fix $\gamma(F)$ in $\gamma(P)$ when $\gamma(P)$ is a cyclic group or a dihedral group. Let the single rotation axis (or the principal axis) of $\gamma(P)$ be a k -fold axis. To fix the arrangement of $\gamma(F)$ in $\gamma(P)$, we first consider an embedding of $\gamma(P)$ to unoccupied rotation axes of $\gamma(F)$. If there are multiple ways to embed $\gamma(P)$, we select an embedding where the single (or principal) rotation axis of $\gamma(P)$ corresponds to the maximum fold of $\gamma(F)$. There may be still multiple ways to embed $\gamma(P)$, but the vertices of the reference polygon of P overlap those F . For example, consider the case where $\gamma(P) = C_1$ and $\gamma(F) = T$. In this case, ψ_{PF} embeds C_1 to a 3-fold axis of T , and the arrangement of T does not depend on which 3-fold axis is selected. Algorithm ψ_{PF} realizes such arrangement of $\gamma(F)$ in $\gamma(P)$ by using the specified rotation axes and reference polygons of P and F .

Finally, if embedding of $\gamma(F)$ to $\gamma(P)$ does not fix \tilde{F} , ψ_{PF} fixes \tilde{F} by overlapping the reference polygon of F to that to P . For example, when P is a pyramid with a regular k -gon base and F is a pyramid with a regular $2k$ -gon base, ψ_{PF} fixes \tilde{F} by overlapping the regular $2k$ -gon reference polygon of F to the regular k -gon reference polygon of P .

6.2 Assigning the final position

Let P and \tilde{F} be a terminal configuration of ψ_{SYM} and the target pattern fixed in P , respectively. The robots now compute a perfect matching between the points of P and the points of \tilde{F} to finally form the target pattern.

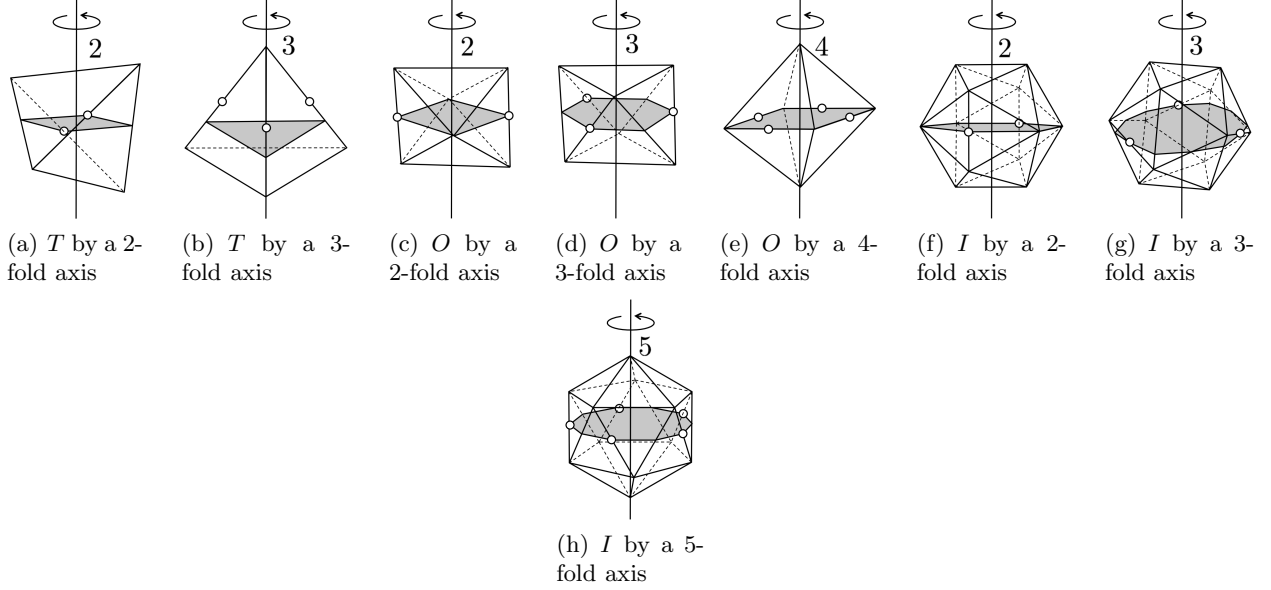


Fig. 30. Reference polygon for T, O, I when one rotation axis is specified. Instead of drawing rotation axes, we show a typical regular polyhedron that shows the arrangement of rotation axes of $\gamma(F)$.

We now consider the rotation group of $P \cup \tilde{F}$. We consider the rotations that matches the points of P to P itself and those of \tilde{F} to \tilde{F} . Hence, $\gamma(P \cup \tilde{F}) \preceq \gamma(P)$. Actually, $\gamma(P \cup \tilde{F}) = \gamma(P)$ because $\gamma(P) \in \varrho(\tilde{F})$ and each $G \in \varrho(\tilde{F}) \preceq \gamma(F)$, i.e., any rotation of $\gamma(P)$ is applicable to \tilde{F} . The group action of $\gamma(P)$ divides $P \cup \tilde{F}$ to a transitive set of points regarding $\gamma(P)$ so that each element consists of only the point of P or only those of F . Additionally, each element consists of $|\gamma(P)|$ points since no robot is on $\gamma(P)$.

Now, in the same way as [21], the robots can order the elements. Let $\{P_1, P_2, \dots, P_m\}$ and $\{F_1, F_2, \dots, F_m\}$ be the elements of P and those of \tilde{F} that appears the entire decomposition in this order. Then, the proposed algorithm makes the robots forming P_i to the positions of F_i for each $1 \leq i \leq m$. In each element P_i , each robot selects the nearest point in F_i as its destination. We first show that there exists a minimum weight perfect matching between the points of P_i and F_i , where the weight is the sum of distances between matched points.

Lemma 13. *For each element P_i and F_i , there exists a minimum weight perfect matching between the points of P_i and the points of F_i .*

Proof. For an arbitrary $p_j \in P_i$, let f_j be one of the nearest point in F_i . Because P_i is transitive regarding $\gamma(P)$ and $|P_i| = |\gamma(P)|$, for each $p_k \in P_i$, there exists $g_k \in \gamma(P)$ such that $g_k * p_j = p_k$, and for any $p_k \neq p_\ell$, $g_k \neq g_\ell$. We apply g_k to f_j so that we obtain the matching point for each $p_k \in P_i$. Because F_i is also transitive regarding $\gamma(P)$ and $|F_i| = |\gamma(P)|$, this procedure produces distinct matching points for each $p_k \in P_i$. Consequently, we obtain a minimum weight perfect matching between P_i and F_i . \square

However, each point of $p \in P_i$ may have multiple nearest destinations. Figure 31 shows an example where P_i forms an expanded cube and F_i forms a truncated cube. For each robot (white circle), there are two nearest destinations (black circles) around the nearest corner of the cube. In this case, we can show that the conflict forms a cycle around a rotation axis and the robots can

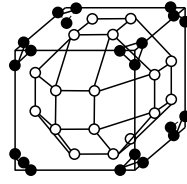


Fig. 31. Minimum weight perfect matching between elements of P and \tilde{F} . The white circles are positions of the robots, and the black circles are the positions of destinations. Thus P forms an expanded cube and \tilde{F} forms a truncated cube. Each robots has two nearest target points.

resolve it by a right-screw rule around the rotation axis. The following lemma shows that we can apply this idea to resolve any conflict.

Lemma 14. *Consider the graph G formed by vertices of $P_i \cup F_i$. For each $p \in P_i$, if $f \in F_i$ is a nearest destination, then we have edge (p, f) . Then, if G contains a cycle, it is around a rotation axes of $\gamma(P)$ and such rotation axis is uniquely determined for each cycle.*

Proof. Clearly, each $p_j \in P_i$ has at least one nearest destination. First, we prove that each $p_j \in P_i$ has at most two nearest points of F_i . Assume p_j has $k > 2$ nearest points of F_i . Then these points are on a circle on $B(F_i)$ and because they are nearest to p_j , no point of F_i is in this circle. Hence these k points are on one face of F_i . Because F_i is transitive set of points, they are on a sphere, these k points form a face of the convex hull of F_i , and p_j is on the line connecting the center of the face and $b(P)$. Because $|F_i| = |\gamma(P)|$, the center of each face of F_i intersects with a rotation axis and p_i is on a rotation axis, which contradicts the fact that $|P_i| = |\gamma(P)|$.

Second, we will show that if $p_j \in P_i$ has two nearest destinations, then there is a cycle in G containing p_j around a rotation axis of $\gamma(P)$. Let f_{j1}, f_{j2} be the two nearest destinations of p_j . Then in the same way as the above discussion, each $p_k \in P_i$ has such two nearest destinations. By the counting argument, there exists at least one $p_k \in P_i$ such that $\{f_{j1}, f_{j2}\} \cap \{f_{k1}, f_{k2}\} \neq \emptyset$. Let $f_{j2} = f_{k1}$. Because P_i is transitive, for p_k , there exists $g_k \in \gamma(P)$ such that $g_k * p_j = p_k$. Then, there exists another point $p_\ell = g_k * p_k \in P_i$ such that $f_{k2} = f_{\ell1}$. By repeating this argument, there exists a subset of P_i that share their nearest destinations. Remember that g_k is a rotation around some rotation axis of $\gamma(P)$. Thus g_k forms a cyclic group and these subsets are around this rotation axis. Thus any cycle in G is around some rotation axis of $\gamma(P)$. Additionally such rotation axis is uniquely determined. \square

For each cycle, the robots can recognize the unique rotation axis that produces the cycle, and they can resolve the conflict by the right-handed screw rule with the positive direction being $b(P)$, i.e., they select the nearest element in the clockwise direction around the rotation axis.

We denote the entire matching obtained by these rules by $M(P, \tilde{F})$. Remember that all computations consisting of finding reference polygon, fixing \tilde{F} , decomposition $P \cup \tilde{F}$, and computing $M(P, \tilde{F})$ is done in one Compute phase in a terminal configuration of ψ_{SYM} . Finally, robots move the corresponding position in $M(P, \tilde{F})$ to complete the pattern formation.

We finally show the proposed pattern formation algorithm ψ_{PF} in Algorithm 6.1.

Algorithm 6.1 Pattern formation algorithm ψ_{PF} for robot $r_i \in R$

Notation

P : The positions of robots observed in Z_i .
 p_i : current position of r_i .

Algorithm

If P is not a terminal configuration of ψ_{SYM} **then**
 Execute ψ_{SYM} .
Else
 Let \tilde{F} be the target pattern fixed in P .
 Move to the matched point in $M(P, \tilde{F})$.
Endif

7 Discussion and conclusion

We have shown a necessary and sufficient condition for FSYNC robots to form a given target pattern. We introduce the notion of symmetricity of positions of robots in 3D-space and used it to characterize the pattern formation problem.

In this section, we consider target patterns with multiplicity and show that we have the same characterization. To define the symmetricity of target patterns with multiplicities, we extend the notion of symmetricity as follows: A multiset of points P is transitive regarding a rotation group $G \in \mathbb{S}$ if it is one orbit regarding G and the multiplicity of point $p \in P$ on a k -fold rotation axis of G is k .

Definition 6. *Let P be a multiset of points. The symmetricity of P , denoted by $\varrho(P)$, is the set of rotation groups $G \in \mathbb{S}$ such that there is an arrangement of G that decomposes P into transitive multisets or transitive sets of points regarding G .*

The above definition adds the decomposition of F into transitive multiset of points when F contains multiplicity. For example, consider a target pattern F whose points occupy the vertices of a cube but each vertex contains three points of F . Thus $|F| = 24$ and $\varrho(F) = \{O\}$. Clearly, from an initial configuration P that forms a truncated cube, the oblivious FSYNC robots can form F by each robot gathering the nearest vertex of the cube. The following theorem directly follows from the discussions through this paper.

Theorem 6. *Regardless of obliviousness, FSYNC robots can form a target pattern F with multiplicity from an initial configuration P if and only if $\varrho(P) \subseteq \varrho(F)$.*

The necessity is clear from the discussion in Section 5. The proposed pattern formation algorithm can be easily extended to target patterns with multiplicity. The only difference is when we consider the $\gamma(P')$ -decomposition of $P' \cup \tilde{F}$ where the robots cannot agree on a unique ordering of the elements formed by \tilde{F} because of the multiplicity. However, this procedure does not require the robots to agree on the ordering of elements formed by \tilde{F} occupying the same positions. The robots just agree on the ordering among the elements formed by P' , and which elements is assigned to such positions with multiplicity.

Our future direction is to consider the pattern formation problem for weaker robot models, for example,

- SSYNC or ASYNC robots,
- Robots with non-rigid movement,
- Robots with limited visibility, and
- Robots without chirality.

Another question is whether there exists a clear separation between the ability of robots in 2D-space and that of robots in 3D-space.

References

1. H. Ando, Y. Oasa, I. Suzuki, and M. Yamashita, Distributed memoryless point convergence algorithm for mobile robots with limited visibility, *IEEE Trans. Robotics and Automation*, 15, 5, pp.818–828, 1999.
2. M.A. Armstrong, Groups and symmetry, Springer-Verlag New York Inc., 1988.
3. M. Cieliebak, P. Flocchini, G. Prencipe, and N. Santoro, Distributed computing by mobile robots: gathering, *SIAM J. Comput.*, 41, 4, pp.829–879, 2012.
4. H.S.M. Coxeter, Regular polytopes, Dover Publications, 1973.
5. P. Cromwell, Polyhedra, University Press, 1997.
6. S. Das, P. Flocchini, G. Prencipe, N. Santoro, and M. Yamashita, Autonomous mobile robots with lights, *Theor. Comput. Sci.*, 609, pp.171–184, 2016.
7. S. Das, P. Flocchini, N. Santoro, and M. Yamashita, Forming sequence of geometric patterns with oblivious mobile robots, *Distrib. Comput.*, 28, pp.131–145, 2015.
8. E.W. Dijkstra, Self-stabilization in spite of distributed control, *Communications of the ACM*, 17, 11, pp.643–644, 1974.
9. A. Efrima and D. Peleg, Distributed algorithms for partitioning a swarm of autonomous mobile robots, *Theor. Comput. Sci.*, 410, pp.1355–1368, 2009.
10. P. Flocchini, G. Prencipe, and N. Santoro, Distributed Computing by Oblivious Mobile Robots, Morgan & Claypool, 2012.
11. P. Flocchini, G. Prencipe, N. Santoro, and G. Viglietta, Distributed computing by mobile robots: Solving the uniform circle formation problem, *In Proc. of OPODIS'14*, pp.217–232, 2014.
12. P. Flocchini, G. Prencipe, N. Santoro, and P. Widmayer, Gathering of asynchronous robots with limited visibility, *Theor. Comput. Sci.*, 337, pp.147–168, 2005.
13. P. Flocchini, G. Prencipe, N. Santoro, and P. Widmayer, Arbitrary pattern formation by asynchronous, anonymous, oblivious robots, *Theor. Comput. Sci.*, 407, pp.412–447, 2008.
14. N. Fujinaga, Y. Yamauchi, H. Ono, S. Kijima, and M. Yamashita, Pattern formation by oblivious asynchronous mobile robots, *SIAM J. Comput.*, 44, 3, pp.740–785, 2015.
15. T. Izumi, S. Kamei, and Y. Yamauchi, Approximation algorithms for the set cover formation by oblivious mobile robots, *In Proc. of OPODIS 2014*, pp.233–247, 2014.
16. D. Peleg, Distributed coordination algorithms for mobile robot swarms: New directions and challenges, *In Proc. of IWDC 2005*, pp.1–12, 2005.
17. I. Suzuki and M. Yamashita, Distributed anonymous mobile robots: Formation of geometric patterns, *SIAM J. Comput.*, 28, 4, pp.1347–1363, 1999.
18. M. Yamashita and I. Suzuki, Characterizing geometric patterns formable by oblivious anonymous mobile robots, *Theor. Comput. Sci.*, 411, pp.2433–2453, 2010.
19. Y. Yamauchi and M. Yamashita, Pattern formation by mobile robots with limited visibility, *In Proc. of SIROCCO 2013*, pp.201–212, 2013.
20. Y. Yamauchi and M. Yamashita, Randomized pattern formation algorithm for asynchronous oblivious mobile robots, *In Proc. of DISC 2014*, pp.137–151, 2014.
21. Y. Yamauchi, T. Uehara, S. Kijima, M. Yamashita, Plane Formation by Synchronous Mobile Robots in the Three Dimensional Euclidean Space, *In Proc. of DISC 2015*, pp.92–106, 2015.

Table 4. Definition of octant

Number	x	y	z
1	+	+	+
2	-	+	+
3	-	-	+
4	+	-	+
5	+	+	-
6	-	+	-
7	-	-	-
8	+	-	-

A Property of rotation groups

Property 1. *Let $P \in \mathcal{P}_n^3$ be a set of points. If D_2 acts on P and we cannot distinguish the principal axis of (an arbitrary embedding of) D_2 , then $\gamma(P) \succ D_2$.*

Proof. Without loss of generality, we can assume that x - y - z axes of the global coordinate system Z_0 are the 2-fold axes of D_2 .¹³ We define the octant according to Z_0 as shown in Figure 32(a) and Table 4.

We consider the positions of points of P in the first octant, which defines the positions of points of P in the third, sixth, and the eighth octant by the rotations of D_2 . The discussion also holds symmetrically in the second octant, that determines the positions of points in the fourth, fifth, and seventh octant.

We focus on a point $p \in P$ and depending on the position of p , we have the following five cases.

- p is on the x -axis (thus, the discussion follows for y -axis and z -axis, respectively).
- p is on the x - y plane (thus, the discussion follows for y - z plane and z - x plane, respectively).
- p is on the line $x = y = z$.
- other cases.

We will show that in any of the four cases, if we cannot recognize the principal axis, then we can rotate P around the four 3-fold axis $x = y = z$, $-x = y = z$, $-x = -y = z$, and $x = -y = z$.

Case A: When $p \in P$ is on the x -axis. Because $\gamma(P) = D_2$, we have a corresponding point on the negative x -axis (Figure 32(b)). This allows us to recognize the x -axis from the y -axis and z -axis, hence P should have corresponding points on y -axis and z -axis. In this case, we can rotate the corresponding six points around the four 3-fold axes.

Case B: When $p \in P$ is on the x - y plane. First consider the case where a point $p \in P$ is on the line $x = y$. Because $\gamma(P) = D_2$, we have four corresponding points on the x - y plane that forms a square (Figure 32(c)). This allows us to recognize the z -axis from the other two axes, hence y - z plane and z - x plane also have the corresponding squares. Hence, the twelve points form a cuboctahedron, and we can rotate them around the four 3-fold axes.

When p is not on the line $x = y$, because $\gamma(P) = D_2$, we have four corresponding points on the x - y plane that forms a rectangle (Figure 32(d)). This allows us to recognize the principal axis. In the same way as the above case, there are two rectangles on the y - z plane and z - x plane. The obtained polyhedron consists of 12 vertices and we can rotate it around the four 3-fold axes.

¹³ There exists a translation consisting of rotation and translation that overlaps the 2-fold axis of $\gamma(P)$ to the three axes.

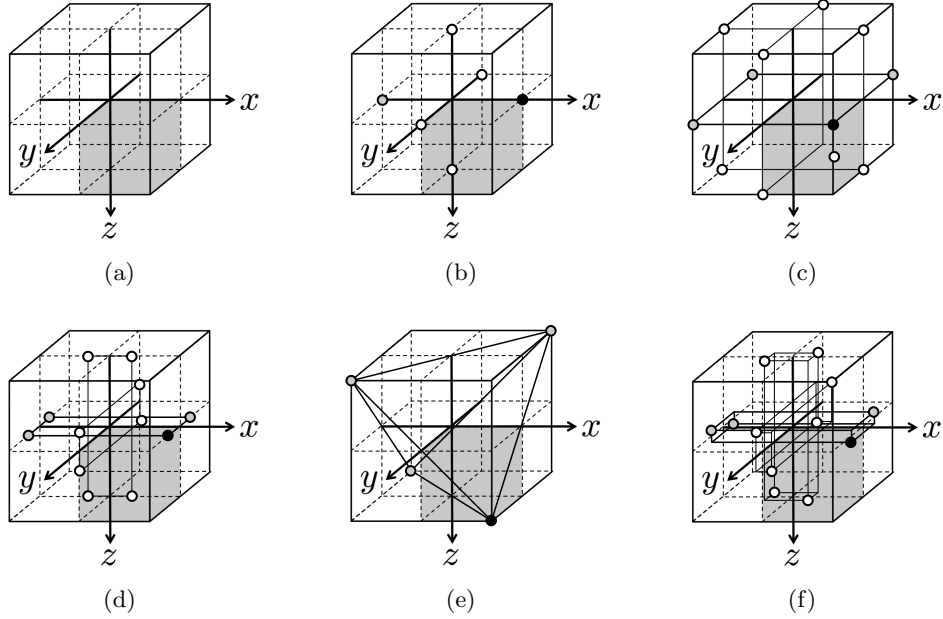


Fig. 32. Position of a point of P in the first octant, and the corresponding points generated by the D_2 . The first octant is shown in the gray box in (a). The black circle is a point of P , and the gray circles are the points generated by D_2 . The white circles are generated so that none of the three rotation axes is recognized.

Case C: When $p \in P$ is on the line $x = y = z$.

Because $\gamma(P) = D_2$, we have four corresponding points in the third, sixth, and the eighth octant, that forms a regular tetrahedron (Figure 32(e)). In this case, we can rotate the corresponding four points around the four 3-fold axes.

Case D: Other cases.

For a point $p \in P$ in the first octant, because $\gamma(P) = D_2$, we have corresponding four points in the third, sixth, and the eighth octant, that forms a sphenoid (Figure 32(f)). This allows us to recognize the z -axis from the others, hence y -axis and x -axis also have the corresponding sphenoids. The obtained polyhedron consists of 12 vertices and we can rotate it around the four 3-fold axes.

Consequently when D_2 acts on P but we cannot recognize the principal axis, we can rotate P around the four 3-fold axes. Thus $\gamma(P) \succeq T$.

□

Clearly, Property 1 holds for the robots since the above discussion does not depend on the local coordinate systems.